MINISTÉRIO DA EDUCAÇÃO
UNIVERSIDADE FEDERAL DO RIO GRANDE DO SUL
PROGRAMA DE PÓS-GRADUAÇÃO EM ENGENHARIA MECÂNICA

EXPERIMENTAL STUDY OF CO-COMBUSTION OF BIOMASS WITH COAL IN A DROP TUBE FURNACE

por

Amanda Tavares de Oliveira

Dissertação para obtenção do Título de
Mestre em Engenharia

Porto Alegre, Agosto de 2022

EXPERIMENTAL STUDY OF CO-COMBUSTION OF BIOMASS WITH COAL IN A DROP TUBE FURNACE

por

Amanda Tavares de Oliveira
Engenheira Mecânica

Dissertação submetida ao Corpo Docente do Programa de Pós-Graduação em Engenharia Mecânica, PROMEC, da Escola de Engenharia da Universidade Federal do Rio Grande do Sul, como parte dos requisitos necessários para a obtenção do Título de

Mestre em Engenharia

Área de Concentração: Energia

Orientador: Prof. Dr. Fernando Marcelo Pereira
Co-Orientadora: Dr. Juliana Gonçalves Pohlmann

Aprovada por:

Prof. Dr. Diogo Elias da Vinha Andrade..... PROMEC / UFRGS

Prof. Dr. Thamy Cristina Hayashi ..... DEMEC / UFRGS

Prof. Dr. Paulo Smith Schneider ..... PROMEC / UFRGS

Prof. Dr. Felipe Roman Centeno
Coordenador do PROMEC

Porto Alegre, Agosto de 2022

CIP - Catalogação na Publicação

Oliveira, Amanda
Experimental study of co-combustion of biomass with coal in a drop tube furnace / Amanda Oliveira. -- 2022.
98 f.
Orientador: Fernando Pereira.

Coorientadora: Juliana Pohlmann.

Dissertação (Mestrado) -- Universidade Federal do Rio Grande do Sul, Escola de Engenharia, Programa de Pós-Graduação em Engenharia Mecânica, Porto Alegre, BR-RS, 2022.

1. Co-combustion. 2. Biomass. 3. Coal. 4. Burnout. 5. Drop Tube Furnace. I. Pereira, Fernando, orient. II. Pohlmann, Juliana, coorient. III. Título.

Elaborada pelo Sistema de Geração Automática de Ficha Catalográfica da UFRGS com os dados fornecidos pelo(a) autor(a).

"Intelligence and education that hasn't been tempered by human affection isn't worth anything."

(Daniel Keyes)

ACKNOWLEDGMENTS

I would like to thank:

My parents Rosemeri and Reinaldo for always prioritizing my education and believing in my dreams. I also thank my brother Léo for encouraging me in all my goals. I could not be here without their support.

My boyfriend Matheus for being by my side throughout the process until the completion of this work, especially when things got tough.

My advisor Fernando and my co-advisor Juliana for all the knowledge shared over these last two years, but especially for trusting my work.

My lab colleagues Natália Jung and Natalia Fenner for their efforts during tireless hours of work in the laboratory and all the support they gave to me this last year. I also thank Roberto, Vitor, and Maira for their contribution to this work.

My classmates, who became friends, Kelly and Augusto for sharing with me the difficulties of the master's degree always with good humor and nice talks.

All professors and faculty members who helped in some way during this period, especially the laboratory technicians Rafael and Henrique for their support.

All my family members and all my friends who believed in me and encouraged me on this journey. I could not mention every single one, but they all mean a lot to me.

I would also like to thank the Braskem team for providing the coal and biomass samples used and for their fundamental contributions to this work.

Finally, I am very thankful for the financial support of the Coordenação de Aperfeiçoamento de Pessoal de Nível Superior (CAPES) for the development of this work.

RESUMO

A matriz energética mundial é constituída principalmente por combustíveis fósseis, sendo o carvão a segunda maior fonte primária de energia. No entanto, os efeitos adversos causados pelas emissões que são geradas durante a conversão de carvão têm causado preocupação nas últimas décadas, enfatizando a necessidade de suprir as demandas energéticas futuras de maneira mais sustentável. A co-combustão de carvão e biomassa tem sido bastante adotada em plantas a carvão como uma maneira de reduzir a emissão de gases do efeito estufa. Sendo assim, o presente trabalho tem como objetivo investigar o impacto da co-combustão com relação à eficiência de combustão (*burnout*) e emissões gasosas. Propriedades físicas e químicas de serragem, cavaco de pinus, cavaco de eucalipto, casca de arroz e bagaço de cana foram avaliadas e duas biomassas foram selecionadas para análise de combustão com carvão brasileiro. As misturas de carvão e biomassa foram preparadas com serragem e bagaço de cana. O estudo experimental foi realizado em um forno de queda livre, amplamente conhecido *Drop Tube Furnace* (DTF). Amostras de *char* foram coletadas em três distâncias axiais ao longo do eixo do forno. O *burnout* das amostras foi calculado pelo método traçador de cinzas. Analisadores de gases foram utilizados para monitorar e gravar as emissões durante os testes de combustão. Inicialmente, foram preparadas misturas com carvão pulverizado e 10% de biomassa (base energética) com partículas de biomassa em tamanhos d < 250 µm, d < 500 µm e d < 1000 µm. As amostras com partículas de serragem de menores tamanhos atingiram *burnouts* estatisticamente iguais ao do carvão puro e convergiram para o *burnout* total no mesmo ponto que o carvão. Contudo, foi observada uma tendência de diminuição no *burnout* para a amostra com partículas de serragem maiores (d < 1000 µm). Em contrapartida, para as misturas com bagaço de cana, foi observada uma tendência de redução do *burnout* também para as amostras com partículas < 500 µm. Essa tendência de diminuição da eficiência de queima foi associada com a grande razão de aspecto das biomassas, que pareceu ter mais impacto no caso do bagaço de cana. Em seguida, foram geradas misturas de carvão com proporções de biomassa de 10%, 20%, 30% e 40% com partículas de biomassa d < 500 µm. Em geral, misturas de serragem com carvão até 40% de biomassa atingiram resultados de queima melhores do que as misturas com bagaço de cana em qualquer proporção. Em geral, emissões de CO e de NO geradas pela combustão de misturas de carvão e bagaço de cana foram maiores que as emissões das misturas de carvão e serragem. As emissões de SO_2 tenderam a reduzir com o aumento da proporção de biomassa nas misturas com os dois tipos de biomassa.
Palavras-chave: Co-combustão; Biomassa; Carvão; Burnout; DTF.

ABSTRACT

The global energy matrix is mainly dominated by fossil fuels, in which coal is the second-largest primary energy source. However, concerns about the adverse effect of the emissions arising from coal conversion have been increasing in the last decades, enhancing the need to meet future energy demands sustainably. Co-firing of coal and biomass in existing coal-fired units is being widely adopted as one of the major technologies for reducing greenhouse gas emissions. This work aimed to investigate the impact of co-combustion of coal and biomass in industrial applications regarding combustion efficiency (burnout) and gaseous emissions. Sawdust, pine chips, eucalyptus chips, rice husk, and sugarcane bagasse had their physical and chemical properties evaluated, and two biomass fuels were selected for combustion analysis with Brazilian coal. Coal-biomass blends were prepared with sawdust and sugarcane bagasse. The experimental investigation was carried out in a Drop Tube Furnace (DTF). Partially burned particles (char) were collected at three axial distances along the furnace axis. The burnout of samples was calculated according to the ash-tracer method. Gas analyzers monitored and recorded gaseous emissions generated during combustion in DTF. Firstly, pulverized coal was mixed with 10% biomass (energy base) with biomass particle sizes of d < 250 µm, d < 500 µm, and d < 1000 µm. For the samples with smaller particles, mixtures with 10% sawdust reached burnout values statistically equal to pure coal burnout and converged to maximum burnout at the same point as coal, but a decreasing trend was observed for combustion of the sample with larger particles (d < 1000 µm). On the other hand, mixtures with 10% sugarcane bagasse showed a tendency to decrease combustion efficiency increasing biomass particle size to < 500 µm. The decrease observed in burnout was associated with the large aspect ratio of biomass, which appeared to cause more impact in sugarcane bagasse samples. After that, sawdust and sugarcane bagasse were blended with coal to generate progressive shares of 10%, 20%, 30%, and 40% of the biomass in the mixture with biomass particles d < 500 µm. Generally, mixtures of sawdust with coal until 40% of biomass share achieved better results during combustion than mixtures of sugarcane bagasse with coal in any proportion. Concerning gaseous emissions, CO and NO emissions from coal-sugarcane bagasse blends were higher than emissions from coal-sawdust blends. Emissions of SO_2 showed a tendency to decrease with the increase of biomass for both coal-sawdust and coal-sugarcane bagasse blends.

Keywords: Co-combustion; Biomass; Coal; Burnout; Drop Tube Furnace.

CONTENTS

LIST OF FIGURES

LIST OF TABLES

LIST OF ACRONYMS AND ABBREVIATIONS

AR6	Sixth Assessment Report
ASTM	American Society for Testing and Materials
BBR	Biomass blending ratio
CAPES	Coordenação de Aperfeiçoamento de Pessoal de Nível Superior
COP26	UN Climate Change Conference
DT	Deformation temperature
DTF	Drop Tube Furnace
EPE	Empresa de Pesquisa Energética
EU	Eucalyptus chips
FC	Fixed carbon
FT	Fluid temperature
GHG	Greenhouse gas
H_2O	Water
HHV	High heating value
HT	Hemispherical temperature
IEA	International Energy Agency
IPCC	Intergovernmental Panel on Climate Change
LASID	Laboratório de Siderurgia
LHV	Low heating value
PI	Pine chips
PM	Particulate matter
PROMEC	Programa de Pós-Graduação em Engenha Mecânica
PSD	Particle size distribution
RH	Rice husk
SATC	Associação Beneficente da Indústria Carbonífera
SB	Sugarcane bagasse
SW	Sawdust
ST	Spherical temperature
TGA	Thermogravimetric Analysis
VM	Volatile matter
UFRGS	Universidade Federal do Rio Grande do Sul
WP	Wood pellet

LIST OF SYMBOLS

Symbols

$(A/F)_{stoic}$	Stoichiometric air-fuel ratio
Ash_{char}	Ash content in the fuel at the distance of sample collection [%]
Ash_{fuel}	Ash content in the fuel at the injection point [%]
C	Carbon content in mass basis in elemental composition [%]
CO_2	Generated carbon dioxide content [kg_{CO2}/kg_{fuel}]
E	Amount of energy generated by a fuel [kJ]
H	Hydrogen content in mass basis in elemental composition [%]
m	Mass [g]
$\dot{m}$	Mass flow rate [g/h]
M	Molar mass [kg/kmol]
N	Molar content [$kmol/kg_{fuel}$]
O	Oxygen content in mass basis in elemental composition [%]
S	Sulfur content in mass basis in elemental composition [%]
W_i	Mass fraction of species *i* in the fuel [kg_i/kg_{fuel}]
X_b	Mass ratio of biomass for coal substitution
$Y_{i,corr}$	Corrected concentration level of species *i* [ppm]
$Y_{i.md}$	Concentration level of species *I* measured during combustion [ppm]
$Y_{O_2,corr}$	Oxygen level for correction [%]
$Y_{O_2,md}$	Oxygen level measured during combustion [%]
Y_{sub}	Ratio of coal substitution on energy basis

Subscripts

$(.)_b$	Related to biomass
$(.)_C$	Carbon
$(.)_{char}$	Related to char
$(.)_{CO2}$	Carbon dioxide
$(.)_{coal}$	Related to pure coal in general
$(.)_{coal,0}$	Related to pure coal before the addition of biomass
$(.)_{fuel}$	Related to fuels in general
$(.)_H$	Hydrogen

$(.)_m$	Related to coal-biomass mixture
$(.)_O$	Oxygen atom
$(.)_S$	Sulfur

1. INTRODUCTION

During the last decades, pulverized coal has been widely used for power generation around the world. In 2021, coal was the largest source of electricity generation and the second-largest source of primary energy in the world. In addition, over 36% of the worldwide electricity was produced from coal in 2019 [IEA, 2021a]. However, coal-fired power generation is currently the largest single source of carbon dioxide (CO_2) emissions, according to the International Energy Agency (IEA), 2021a.

The Intergovernmental Panel on Climate Change (IPCC) published in the Sixth Assessment Report (AR6) that global warming between 1.5 °C and 2 °C will be exceeded during the 21st century unless deep reductions in CO_2 and other greenhouse gas (GHG) emissions occur in the coming decades. This climate change was mainly caused by human activities and has caused many weather and climate extremes around the globe, such as heat waves, heavy precipitation, droughts, and tropical cyclones [IPCC, 2021].

Limiting cumulative CO_2 emissions, reaching at least net zero CO_2 emissions, along with strong reductions in other GHG emissions are the key to limit global warming to specific level at 1.5 °C [IPCC, 2021]. Therefore, during UN Climate Change Conference (COP26), in November 2021, 45 countries have committed to pledges to reach net-zero CO_2 emissions by 2050, including China and India. In addition, Japan, Korean, and China have also committed to stop public funding for building new coal power projects abroad, as stated in IEA, 2021a. Such commitments should have very strong implications for coal consumption.

Since concerns about the environmental impact of coal combustion have increased, industries are making efforts to reduce the emission of pollutants in their daily activities. Among companies that use coal as a source of energy, the replacement of coal by fuels with low-carbon footprint is a potential approach to achieve this goal. Biomass has attractive properties that make its use a viable option for this purpose.

According to the *Empresa de Pesquisa Energética* (EPE), 2021, biomass is a primary non-fossil energy source that can be derived from different organic matter resources such as dedicated energy crops, forestry and agricultural residues, and organic wastes. Biomass is considered a renewable energy source for several reasons, e.g., it is carbon neutral and it has low contents of nitrogen and sulfur compared to coal [Gil and Rubiera, 2019]. Different types of energy can be generated from the chemical energy stored in biomass, like electricity, depending on the thermochemical conversion process applied.

Co-combustion of biomass with coal in existing coal-fired systems is a widespread practice for using biomass in the power generation industry. Some relevant aspects of co-firing coal and biomass are related to biomass potential in mitigating GHGs, nitrogen oxides (NOx), and sulfur oxides (SO_x) emissions compared to pure coal combustion. Another advantage of co-firing is burning biomass efficiently in existing coal-fired units with minimum modification. However, biomass has high levels of alkali and chlorine in its composition, which may cause an increase in slagging and corrosion effects during biomass burning [Agbor, Zhan and Kumar, 2014]. Therefore, understanding the combustion behavior of biomass before its application in industrial systems is crucial.

The drop tube furnace (DTF) has been used in laboratory experiments to evaluate the potential application of biomass to existing pulverized coal units. The most relevant aspect of DTF for experimental investigations is its capacity to adequately simulate the combustion behavior in industrial equipment, in particular the high temperatures, the high heating rates, and the short residence times. Some important combustion characteristics can be identified from experimental analyses in DTF, such as combustion efficiency (burnout) of fuels and composition of flue gases. Such information can give a useful overview of the impact of biomass in co-firing. A few years ago, a DTF was constructed in the Laboratório de Combustão, in the Universidade Federal do Rio Grande do Sul, to investigate the combustion behavior of solid fuels.

1.1 OBJECTIVES

The present work was developed in partnership with the petrochemical complex of the company Braskem in Triunfo – RS as part of a feasibility study of partial replacement of mineral coal by biomass in Braskem's boilers. Braskem elected five biomass fuels to have their physical and chemical properties investigated. Two of them were selected to have their combustion characteristics studied during co-combustion with coal in the DTF from the Laboratório de Combustão. Therefore, this work aims to investigate the effects of partial substitution of coal by biomass in industrial furnaces using the DTF to perform experimental analysis.

The specific objectives of the study are meant to:

- Evaluate the physical and chemical properties of the fuels;
- Investigate effects of different biomass particle sizes on combustion efficiency;
- Investigate the impact of biomass ratios on burnout along the furnace axis;
- Evaluate the impact of the coal substitution on gaseous emissions.

2. LITERATURE REVIEW

2.1 SOLID FUELS

Solid fuels refer to various solid materials that can be used for energetic purposes, and coal is the best known and most used worldwide. However, many other solid fuels are obtained from different raw materials, such as wood, biomass, and municipal wastes, which have been also called solid biofuels. The characteristics of solid fuels vary widely regarding composition depending on their origin. Generally, solid fuels are composed of carbon, hydrogen, oxygen, water, nitrogen, and ash [Suárez-Ruiz, Diez and Rubiera, 2019].

2.1.1 Coal

According to Suárez-Ruiz, Diez and Rubiera, 2019, coal is an organic and combustible sedimentary rock considered a non-renewable because millions of years are required to form coal. Formation of coal consists of biochemical and geochemical stages. During the biochemical step, bacteria and fungi in a waterlogged environment decompose the plant material, eventually forming peat, which is soft, spongy sediment. This process is called peatification. During the geochemical stage, the peat goes through intermittent subsidence, followed by sedimentation. Over millions of years, much slower chemical changes take place in the buried layers of peat, transforming peat into coal. This process is called coalification [Merrick, 1984].

Coal consists of moisture, volatiles, mineral matter, and carbon-based char, in variable proportions. Depending on the composition of coal, it may be constituted mainly of non-combustible material, that is, moisture and mineral matter [Turns, 2012]. Some of the moisture can be removed by drying in air, as stated in Merrick, 1984. Then, only the inherent moisture remains, which is generally lower than 10 percent. The same occurs with the mineral matter. Part of mineral matter are discrete particles remnant of adjacent strata, or other types of dirt, that can be removed during coal preparation. The inherent mineral matter is composed of fine particles distributed throughout the coal, which makes their removal quite restricted. The type and properties of the inherent material matter depend on the location and mining methods [Merrick, 1984]. On the other hand, the volatiles and char are responsible for the proper energy value of the coal. The main components of the organic matrix of coal are carbon, hydrogen, oxygen, nitrogen, and sulfur [Barbieri, 2013].

Heat and pressure over a period have a major influence on the degree of coal metamorphism, called the coal rank. This metamorphism involves a progressive decrease in moisture and volatile content in coal, consequently increasing its carbon content [Suárez-Ruiz, Diez and Rubiera, 2019]. The heat is considered the most important factor because the temperature of rock strata increases with depth; therefore, the oldest coals have been subjected to the highest temperatures and, consequently, to the greatest chemical changes [Merrick, 1984]. The categories used to describe coal rank are lignite, sub-bituminous coals, bituminous coals, and anthracites, with the order they are mentioned following from the youngest to the oldest coal, as shown in Figure 2.1.

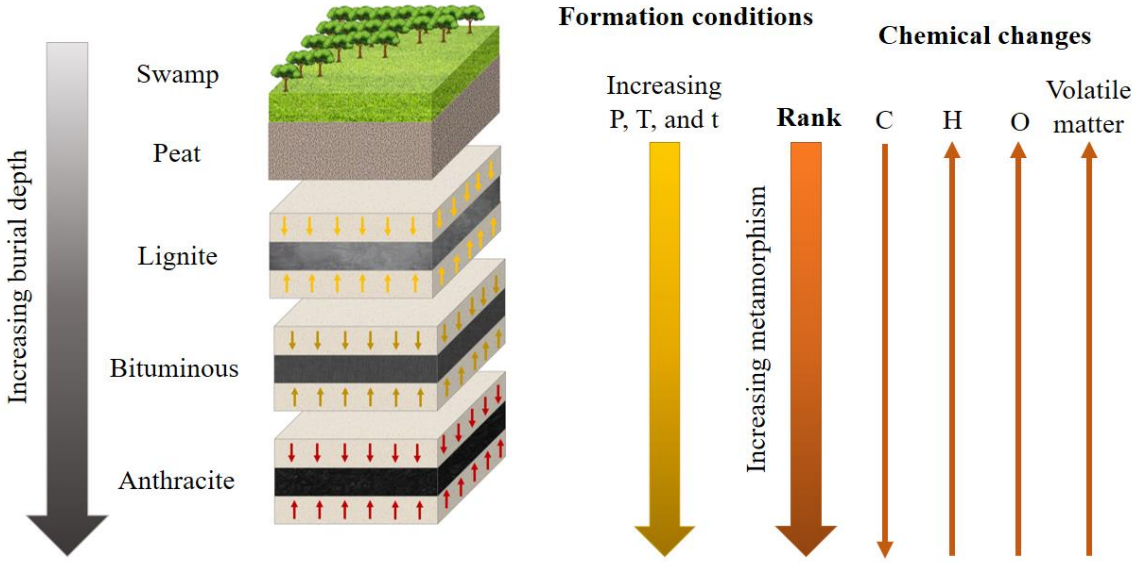

Figure 2.1 – Scheme of formation of coal in terms of rank [Adapted from Suárez-Ruiz, Diez and Rubiera, 2019].

According to the World Coal Association, 2020, there is over 1.06 trillion tons of proven coal reserves worldwide and the biggest reserves are in the United States, Russia, China, Australia, and India. The global consumption and production of coal increased until 2013 when both reached their maximum levels because of the increase in coal consumption by countries of the Asian region. After that, the consumption and production of coal slightly decreased over the years, especially because some important countries are reducing the use of coal as a source of power generation, such as the United States. On the other hand, China and India account for two-thirds of the global coal consumption. Therefore, global trends depend heavily on

developments in Chinese electricity system, which is closely linked to the economic growth in the country. Figure 2.2 shows the coal demand in the last 20 years in the world by region. While coal power generation is disappearing or becoming negligible in many European Union countries, partially because of lower natural gas prices and higher CO_2 prices, coal consumption has increased in India in 2021 due to the economic recovery after Covid-19 lockdowns and a decline in generation from hydro. In fact, China is committed to achieving carbon neutrality by 2060, but their five-year plan (2021-2025) still considers coal an irreplaceable energy source [IEA, 2021b].

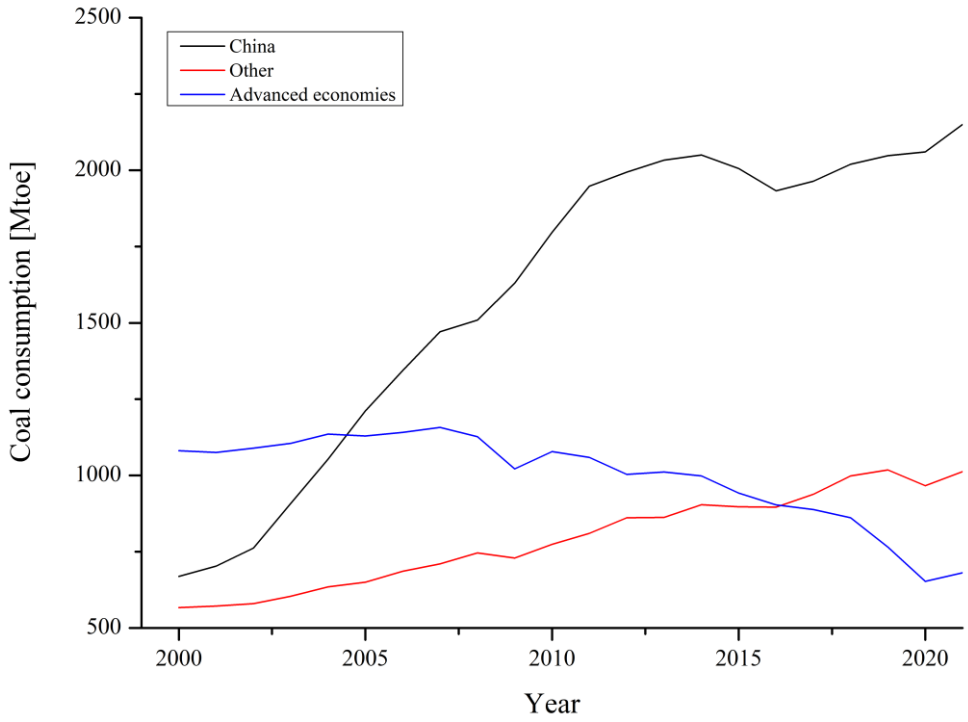

Figure 2.2 – Coal consumption by region, 2000 to 2021 [Adapted from IEA, 2021b].

In Brazil, the energy matrix of the country is 48.3% composed of renewable sources. Concerning electricity generation, renewable sources accounted for 84.8% of the Brazilian domestic supply of electricity in 2020, with emphasis on the water source, which accounted for 65.2% of the domestic supply [EPE, 2021]. A comparison of Brazil's energy matrix and world's energy matrix is presented in Figure 2.3. However, Roni et al., 2017, reported that Brazil has a huge energy potential of agricultural residues since the country produces annually a large amount crops that result in organic residues such as soy, rice, wheat, and sugarcane. Co-firing Brazilian coal with biomass could reduce the impact of ash-related issues in typical combustion

processes because Brazilian biomass usually contains very low ash content. However, most agricultural residues produced in Brazil are located far from the existing coal power plants, which makes biomass co-firing economically unfeasible in coal plants. According to Gomes et al., 1998, Brazilian coal deposits are located in the South region of the country, in the States of Paraná, Santa Catarina, and Rio Grande do Sul, the latter being the one with approximately 90% of the proven reserves.

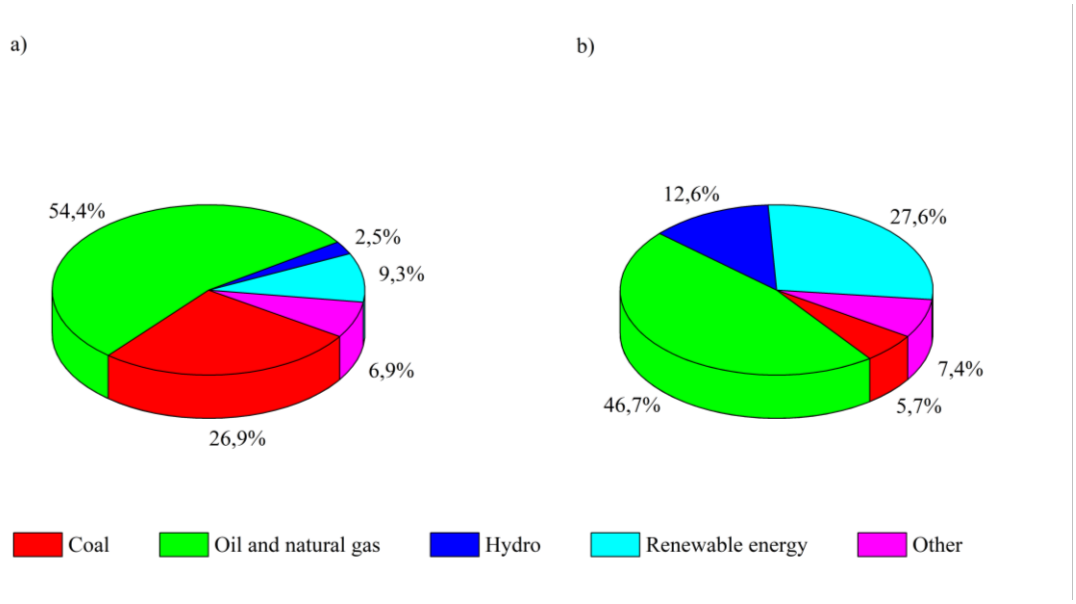

Figure 2.3 – Energy supply by source: (a) global, (b) Brazil [Adapted from EPE, 2021].

Coal has many different and important uses worldwide, in which power generation, steel production, cement manufacturing, and as a liquid fuel stand out. The main processes involved in coal conversion are combustion, gasification, liquefaction, and carbonization [Suárez-Ruiz, Diez and Rubiera, 2019].

2.1.2 Biomass

The characteristics of biomass vary widely depending on the type and category of biomass nature, which includes energy crops (crops harvested solely for their energy content), waste from food crops, waste or by-products from forest products, animal wastes, and many others. The main categories of biomass fuels are exhibited in Figure 2.4. Compared to coal, biomass properties, composition and energy content vary significantly. Conforming to Demirbas, 2005, in terms of elemental composition, biomass usually contains less carbon, more hydrogen and

oxygen, and lower sulfur and nitrogen content than coal. In addition, biomass has less fixed carbon, more volatiles, lower ash content and bulk density than coal. These differences are crucial to understanding the combustion behavior of biomass when burning it in co-combustion with coal. For example, small quantities of sulfur and nitrogen in the fuel may indicate a reduction in nitrogen and sulfur oxides emissions.

Because of the higher proportions of hydrogen and oxygen, biomass fuels tend to have smaller heating values than coal, which is a critical property because it represents the amount of energy available per kg of fuel. However, Sami, Annamalai and Wooldridge, 2001, emphasized that this information is not sufficient to predict biomass combustion efficiency, which is, in turn, a result of both heating value and chemical composition. Therefore, it is possible to have biomass burning with higher combustion efficiency than coal, even though biomass has a smaller heating value.

Another difference between biomass and coal is the composition of their ashes. While coal ash consists mainly of an aluminosilicate system, biomass ash is rich in sodium and potassium, which can reduce the melting point of ash leading to the formation of slagging and fouling on heat exchangers surfaces [Zuwala and Lasek, 2017]. Therefore, ash analysis is essential to predict the combustion behavior of the fuels. However, biomass usually has little ash content compared to coal, so the impact of a different ash composition may be insignificant in the co-combustion of coal with a small amount of biomass.

There are several reasons why biomass is considered environmentally friendly besides that it is considered carbon neutral. One of them is that using biomass residues rather than energy crops in combustion processes helps mitigate the release of methane (CH_4) from the otherwise landfilled biomass. Concerning global warming impact, CH_4 is 21 times more potent than CO_2 [Sahu, Chakraborty and Sarkar, 2014].

Nevertheless, there are some technological and logistical issues associated with the use of biomass in combustion processes. In terms of fuel properties, the lower heating value and the lower bulk density of biomass implicate in a need to transport large amounts of biomass to supply the same energy demand as coal. Therefore, the cost of biomass depends on not only the feedstock origin, type, and composition but also on the cost to handle, prepare, and transport the feedstock. The seasonality of biomass resources can be another obstacle to its use since the feedstock supply is unpredictable [Agbor, Zhan and Kumar, 2014]. These issues will be discussed in more detail later in this work.

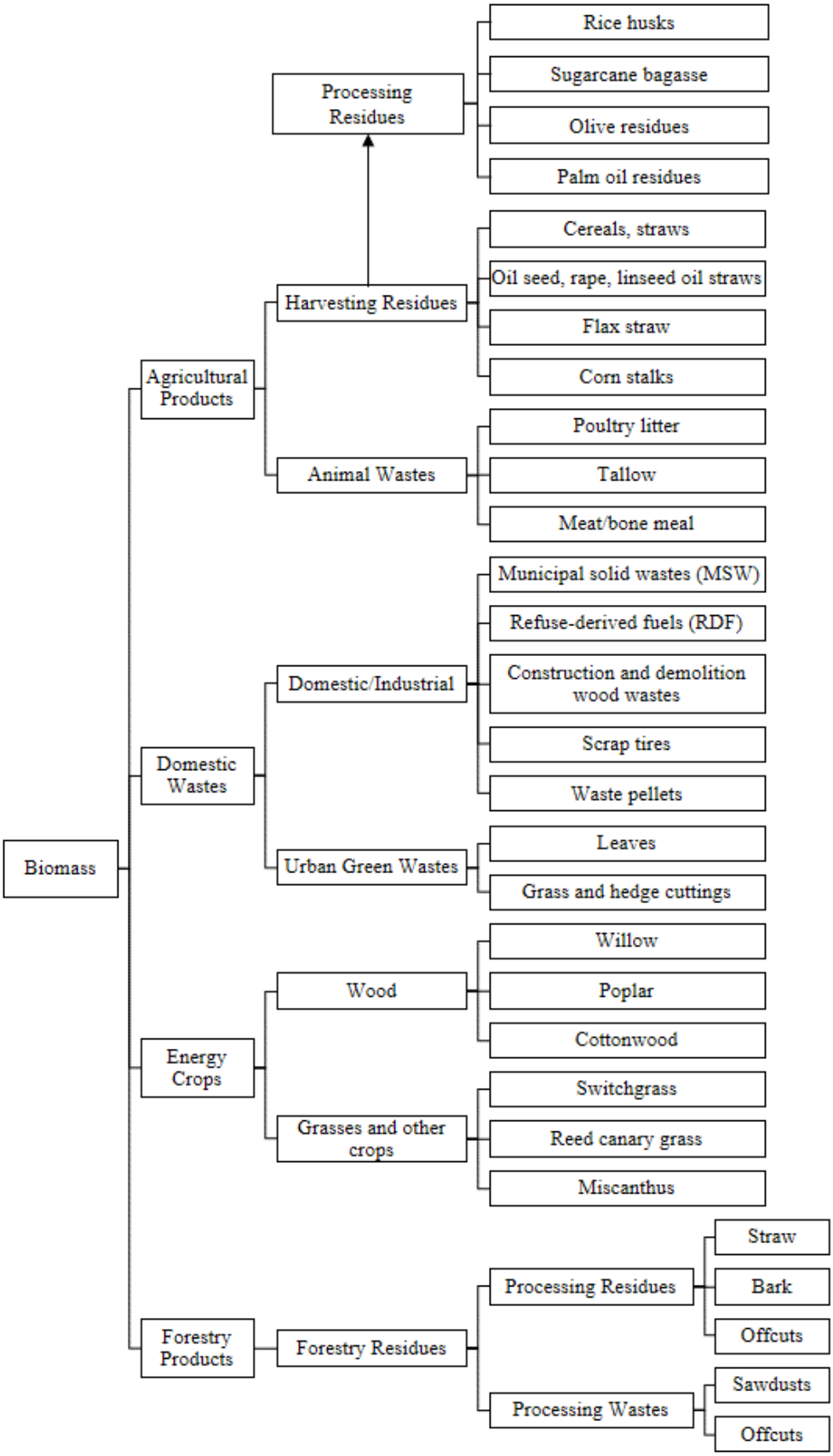

Figure 2.4 – Solid biomass materials of industrial interest [Adapted from Agbor, Zhan and Kumar, 2014].

2.1.3 Combustion process

The combustion process of solid fuels is quite complex compared to the combustion of gaseous or liquid fuels. During the combustion of gases and liquids, only homogeneous reactions are observed while in the combustion of solid fuels heterogeneous reactions appear, which means species in different physical states are involved, specifically gas-solid reactions [Turns, 2012]. Coelho and Costa, 2007, reported that the combustion process of solid fuels generally experiences the following steps: heating and drying of fuel particles, devolatilization, homogeneous oxidation of volatiles, and heterogeneous oxidation of char. The steps do not follow a specific order, which means some steps may occur at the same time.

The heating and drying are endothermic processes controlled by heat and mass transfer, so temperature and particle dimension are essential variables in these processes. During the drying process, particles are heated to approximately 105 °C, the temperature at which the moisture changes to the gaseous state and is released through the pores of the particles [Coelho and Costa, 2007].

Glassman, Yetter and Glumac, 2015, defined the devolatilization process as releasing gaseous fuel components when the solid fuel is heated. These gaseous components correspond to the volatile matter present in the fuel. The devolatilization is followed by the homogeneous oxidation of these volatiles. After volatiles are released from the fuel particle and burned, the remaining matter in the fuel is the char. The volatiles burn faster than char particles, which is relevant for flame ignition and stability and nitrogen oxides formation. The temperature at which devolatilization starts depends on the fuel type. For example, in coals, this temperature is usually between 300 and 400 °C while in biomass fuels it is generally between 200 and 260 °C [Coelho and Costa, 2007]. The total quantity of volatiles released also depends on the fuel's nature, the heating rate, and the final temperature of particles.

The char is a porous residue mainly composed of carbon and mineral matter (ash), and its oxidation occurs through surface reactions of species such as oxygen (O_2), water (H_2O), and carbon dioxide; these reactions can be controlled by either the surface reaction rates (chemical kinetics) or the diffusion of oxygen and they are much slower than devolatilization. There are three zones of combustion to determine which mechanisms are responsible for char oxidation. In Zone I, temperatures are relatively low, and the combustion is controlled by kinetics because the oxygen diffusion is quick. In Zone II, there is an increase in temperature, and the combustion occurs with partial penetration of oxygen, so both effects of the surface reaction rate and the diffusion of oxygen determine the combustion rate. In Zone III, high temperatures arise, and

the surface burning rate is so fast that oxygen is entirely consumed at the surface without penetrating the particle [Glassman, Yetter and Glumac, 2015].

2.1.4 Environmental issues

Climate change associated with human activities has become a worldwide concern in the 21st century. Therefore, pollutant control is a relevant factor in combustion systems development. Pollutants associated with combustion include particulate matter, sulfur oxides, unburned and partially burned hydrocarbons, oxides of nitrogen, and carbon monoxide (CO). In addition, the emission of greenhouse gases is known to be the principal contributor to climate change. Thus, greenhouse gases related to the combustion of fossil fuels, such as carbon dioxide, methane, and nitrous oxide (N_2O), are also receiving attention [Turns, 2012].

Glassman, Yetter and Glumac, 2015, classified air pollutants into two categories. Primary pollutants are emitted directly to the atmosphere, such as unburned hydrocarbons, NO, particulates, and sulfur oxides. Secondary pollutants are formed by chemical and photochemical reactions of primary pollutants when they are exposed to the sunlight in the atmosphere. Some examples of secondary pollutants are peroxyacetyl nitrate and ozone. Some pollutants can be in both categories. For instance, nitrogen dioxide is emitted directly from combustion exhaust and is also formed from nitrogen monoxide (NO) in the atmosphere.

Merrick, 1984, discussed some of the pollutants from coal combustion and their effects on the environment and human health. The author defined that particulate matter emissions can be either in the form of smoke or dust and sand. The smoke corresponds to particles of carbon (soot) and tar fog resulting from incomplete combustion of coal while the dust and grit are essentially coal ash. Both types of particulate matter emissions can be related to health hazards such as respiratory diseases, being the worst effects of smoke emissions. Regarding the emission of sulfur oxides, the author established that sulfur is present in coal as part of the organic coal substance as well as an inorganic compound in the mineral matter. Both organic and inorganic sulfur is released into the atmosphere when coal is burned, mainly in the form of sulfur dioxide. In addition to being associated with respiratory diseases, sulfur dioxide emissions can be responsible for some adverse environmental effects such as corrosion of materials and reduced growth rates of crops. Other relevant effects derive from sulfates because of their acidity, which can result in acid rains. Concerning nitrogen oxide emissions, the environmental impacts are, to some extent, similar to that of sulfur dioxide. Nitrogen oxide arises from the nitrogen present in the coal and atmospheric nitrogen.

Turns, 2012, summarized the role of greenhouse gases in climate change as the absorption of outgoing infrared radiation from the earth increasing the earth's surface temperature. Carbon dioxide in the atmosphere has great relevance in this effect. Changes in the magnitude of global temperature have a huge impact on the global climate and agriculture. For example, global warming may increase the frequency and intensity of hot extremes, marine heatwaves, heavy precipitation, agricultural and ecological droughts; and reductions in Arctic sea ice, snow cover, and permafrost [IPCC, 2021].

2.2 CO-FIRING OF COAL AND BIOMASS

Co-firing coal and biomass consists of burning biomass along with coal in coal-fired power plants. Reducing the environmental impact associated with the combustion of fossil fuels is one of the main reasons to investigate and promote biomass co-firing. However, coal and biomass have quite different natures, which can result in some challenges to adapt an existing system for co-combustion. It is crucial to understand how the configuration of co-firing can affect the combustion process and which one is more suitable for the type of biomass selected. Besides, there are a few technical and logistical issues associated with co-firing that must be considered before choosing the biomass for this process.

2.2.1 Configurations of co-firing

Al-Mansour and Zuwala, 2010, listed three basic configurations for co-firing biomass with coal in coal-fired boilers: direct co-firing, indirect co-firing, and parallel co-firing. Differences in these configurations are related to the boiler system design and the percentage of biomass to be co-fired.

Direct co-firing consists of feeding biomass directly into the furnace after being milled, and then the fuel mixture is burned. The milling process of biomass can occur along with coal in the same mill or individually in a different mill, as shown in Figure 2.5. This configuration is the cheapest and most commonly applied method in co-firing biomass with coal. In addition, it was estimated that no significant additional costs are required when biomass fraction is approximately 3% (energy based) or less [Zuwala and Lasek, 2017]. However, higher capital investment is required when more modifications are introduced to the original system.

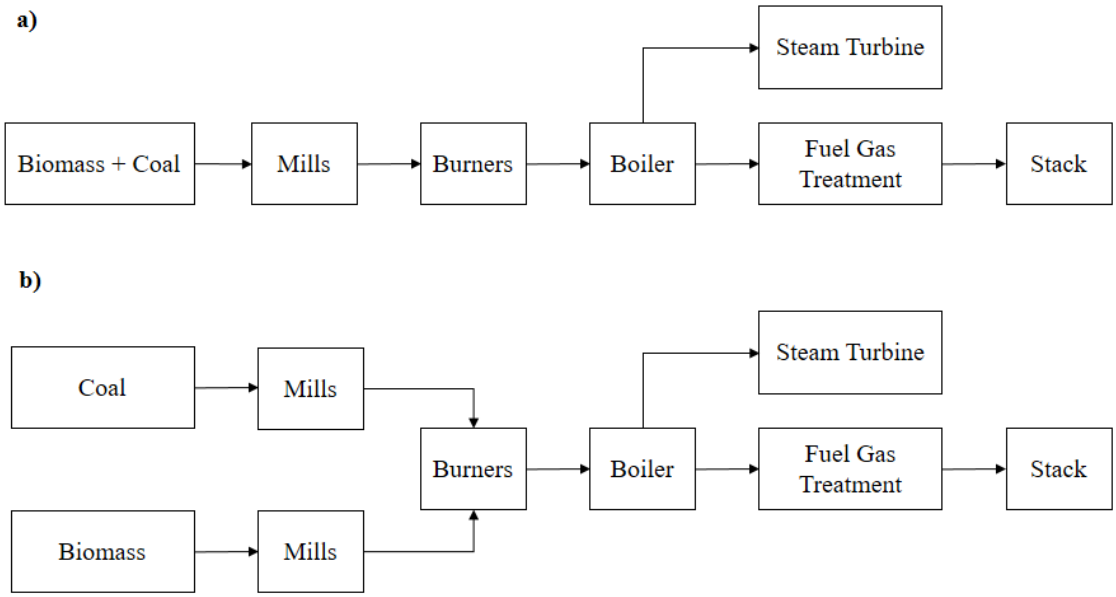

Figure 2.5 – Scheme of direct biomass co-firing technologies: (a) premixed fuel; (b) separate fuel feeding arrangement [Adapted from Agbor, Zhan and Kumar, 2014].

In indirect co-firing, the biomass is submitted to gasification in a separate gasifier before being fed into the furnace, as show in Figure 2.6. This process converts the solid fuel into a fuel gas, which is then burned in the boiler with the base fuel. This method allows a high degree of fuel flexibility in terms of fuel type and percentage of biomass to be used [Al-Mansour and Zuwala, 2010]. In addition, indirect co-firing can also reduce slagging because the fuel is not directly fed into the coal furnace, as stated by Gil and Rubiera, 2019.

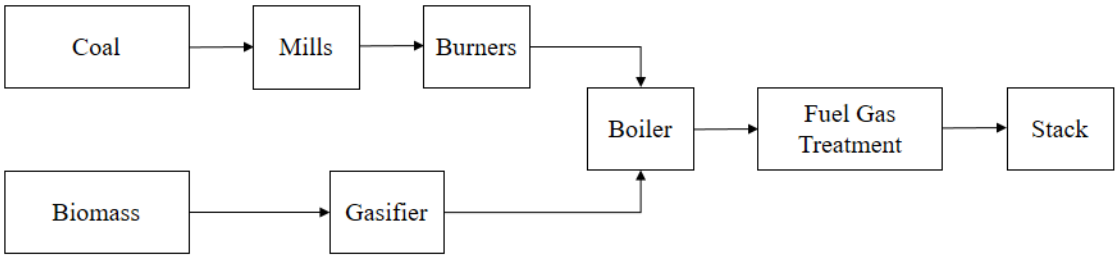

Figure 2.6 – Scheme of indirect co-firing biomass technologies [Adapted from Agbor, Zhan and Kumar, 2014].

In parallel co-firing systems, coal and biomass are handled, fed, and burned in separate systems. Then, the steam generated from biomass burning is mixed with the steam generated from the conventional system, as shown in Figure 2.7. This method allows higher percentages of biomass to be co-fired and offers less risk and more reliability due to the dedicated biomass system. However, parallel co-firing is a technology that requires more capital investment [Agbor, Zhan and Kumar, 2014].

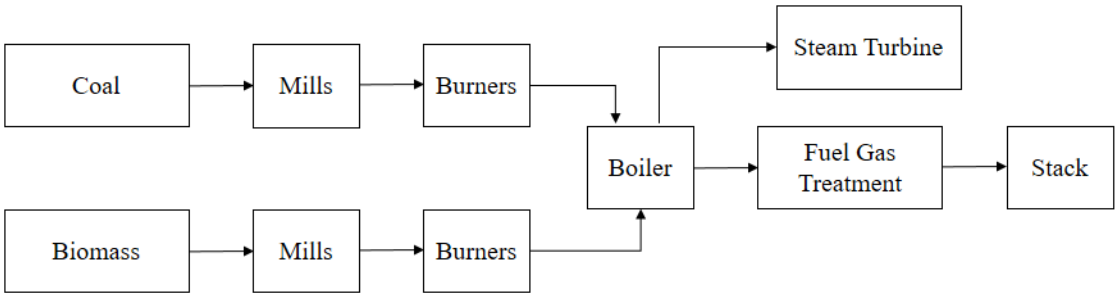

Figure 2.7 – Scheme of parallel co-firing biomass technologies [Adapted from Agbor, Zhan and Kumar, 2014].

2.2.2 Technical and logistical aspects of co-firing

Baxter, 2005, listed the principal technical challenges associated with biomass co-firing: fuel preparation, storage, and delivery, ash deposition, fuel conversion, pollutant formation, corrosion, fly ash utilization, impacts on selective catalytic reduction systems, and formation of striated flows. Some of them will be discussed next.

2.2.2.1 Fuel preparation, storage, and delivery

Because of the biomass fibrous nature and large aspect ratio, its particles have very low packing densities. Therefore, this low bulk density of biomass fuels is one of its characteristics that has a high impact on its preparation, storage, and delivery. The overall biomass density is about one-tenth that of coal, which means that co-firing biomass at a 10% heat input rate has a volumetric flow rate of biomass comparable to coal in magnitude [Baxter, 2011]. Therefore,

the heat contribution of biomass is low compared to the costs of transportation, storage, and handling technologies needed to get biomass prepared for combustion. In general, preparing and handling biomass as a separate fuel is better than mixing it with coal. In addition, the larger size of biomass particle makes its grinding difficult and expansive [Yadav and Mondal, 2019].

Biomass price depends on the fuel nature, including its type and composition, and the plant's geographic location, because the heating value of biomass feedstock influences the transportation cost over long distances. According to Gil and Rubiera, 2019, transportation costs can be reduced by subjecting the biomass to pretreatment techniques, such as biomass densification as pellets and briquettes, or torrefaction. These techniques involve changing raw biomass by reducing its moisture content and increasing the heat value per volume of fuel, which improves its transportation and storage. However, the addition of any technology in the process implies an extra cost in biomass utilization to be considered.

2.2.2.2 Biomass conversion

The large and non-spherical aspects of biomass particles represent a considerable challenge for fuel conversion efficiency. However, biomass has properties that compensate for such an adverse effect because of its shape. Biomass particles can have larger size than coal for the same residence time due to the higher volatile content and reactivity of biomass, as reported by Riaza, Gibbins and Chalmers, 2017. For the conditions established for their experiment, the authors concluded that coal particles in the range of 300-355 μm had similar burnout times to biomass particles in the range of 600-1000 mm.

Coal particles of the same actual size of raw biomass would not burn completely in a boiler under similar conditions because they are very dense, so they would heat up far more slowly. Moreover, biomass particles oxidize at higher rates than coal because of their low densities. Despite these mitigating effects, high moisture content or excessive large particle size of biomass can still pose conversion problems for biomass co-firing [Baxter, 2005].

2.2.2.3 Ash deposition and corrosion

The combustion efficiency of a system can be highly affected by both ash deposition and corrosion. Ash deposition rates from biomass can be either greater or considerably lower than coal depending on the fuels origin. Nonetheless, deposits from biomass are denser and more

difficult to remove than deposits generated during coal combustion [Sami, Annamalai and Wooldridge, 2001].

Basu, 2006, stated that fouling is likely to occur on boiler tubes due to evaporation of alkali salts present in biomass ash, reducing heat transfer to the tubes. Deposition on the tubes reduces steam temperature and increases the metal temperature, which could cause corrosion and erosion problems on combustor surfaces. In addition, the presence of chlorine in combustion gases can also accelerate corrosion in the combustion system, especially on superheaters at high temperature. Chlorine reacts with alkali metals to form low temperature melting alkali chlorides, resulting in a sticky deposition that reduces heat absorption on superheater tubes.

According to Baxter, 2011, the interaction between alkali from the biomass, mainly potassium, and sulfur from the coal causes the mitigation of chlorine-based corrosion in boiler deposits from biomass. Under oxidizing conditions, alkali chlorides that condense from biomass flue gases react with sulfur dioxide, generated primarily from coal, to form alkali sulfates, which are significantly less corrosive. Under a reducing environment, chlorides are formed instead of sulfates, so the mitigation of the corrosion effect does not occur in regions of boilers where deposits are exposed to this condition.

2.2.2.4 Pollutant formation

Sahu, Chakraborty and Sarkar, 2014, investigated some pollutant emissions from coal-biomass co-combustion. Regarding SOx emissions, the author concluded that such emissions often follow a direct relation to the sulfur content in the fuel. Therefore, SOx emissions from co-firing biomass usually decrease in proportion to the thermal load because of the lower sulfur content of biomass. Moreover, alkali and alkaline earth metals present in biomass ash can retain part of SOx emissions, resulting in an additional reduction beyond the amount expected based on the fuel sulfur content. On the other hand, NOx emissions are relatively complicated to anticipate. The author stated that NOx emissions from biomass co-firing could be either higher or lower than those of coal. For example, low-nitrogen woody biomass typically produces much lower NOx. In addition, the higher volatile content of biomass can be used as an advantage to reduce NOx emissions because biomass can create a large fuel-rich region useful for NOx control.

Conforming to Yadav and Mondal, 2019, particulate matter (PM) emission depends strongly on the biomass blending ratio, type, and composition of coal. However, there is some

divergence concerning the behavior of particulate matter emissions from co-firing coal and biomass. Both the increase and the reduction of particulate matter were observed with the increase of the biomass share in studies reported by the authors. Jiang et al., 2022, investigated PM emissions from co-firing two types of bituminous coal with two types of woody biomass in a DTF. Four blends were prepared by cross combination of the fuels. While the PM emissions from two blends increased with increasing the biomass share, PM emissions from the other two blends barely changed compared to single coal combustion.

2.2.3 Operational experience of co-firing worldwide

Biomass co-firing has been demonstrated in over 229 biomass co-firing installations operating worldwide for most combinations of fuels and boilers types typically in the range from 50 MWe to 700 MWe, although a few units are between 5 and 50 MWe [IEA Bioenergy, 2017]. Of those, more than 170 plants are located in different countries in Europe, especially in Finland, while 40 plants are in the United States. The power stations are mainly equipped with pulverized coal boilers in many configurations, but fluidized bed boilers and cyclone boilers are also found in those installations. Blends of coal and biomass include every commercially significant fuel type, such as lignite, sub-bituminous, and bituminous coal, as well as principal categories of biomass fuels, such as herbaceous and woody fuels and energy crops.

Pedersen et al., 1996, investigated the effects of biomass co-firing at the Amager Power Plant Unit 3 (AMV3), a 250 MWe pulverized coal-fired unit in Denmark. The tests were carried out for 1-week using blends of a Canadian high sulfur bituminous coal with 10-20% straw (thermal basis). The authors did not observe severe problems sustaining a stable flame during combustion or occurring deposition on heat transfer surfaces. Straw pellets and coal were mixed before entering the coal mills, and no blockage occurred in the roller mills during grinding. They also investigated the degree of burnout achieved during the test period and identified similar residence times at similar profile temperatures in the furnaces for both coal and coal-straw blend firing. The unchanged combustion efficiency was associated with several factors by the authors, such as particle size distribution, which was coarser with the addition of straw, fuel reactivity, local O_2 concentrations, and the temperature-time history of the particles. In addition, the study indicated that a net reduction of NO and SO_2 emissions could be obtained by blending up to 20% straw with the Canadian coal. The reduction of NO emissions was associated with the lower overall fuel-N conversion, and it was validated by gas-phase

measurements of NO. The reduction of SO_2 emissions with the rising in the straw fraction was attributed to the high potassium content of straw, which can cause sulfur retention.

Savolainen, 2003, evaluated the impact of co-firing pine sawdust with coal at FORTUM's Naantali-3 CHP power plant regarding boiler performance, flame stability, and emissions. The tests were carried out for three months using blends of coal with sawdust proportions of 2.5-8% (from the fuel input). Coal and sawdust were mixed in the coal yard before being fed into the boiler through the existing coal mills. The performance of the coal mills was a limiting factor defining the maximum proportion of sawdust in co-firing because the mill capacity and the boiler capacity were limited with high shares of sawdust. In addition, grinding coal and sawdust in the same roller mills negatively affected the coal fineness results, increasing the number of coarse particles and reducing the amount of smaller ones, leading to a reduction in the burnout efficiency of coal. The ignition and the flame stability were noticed to be typical during all the tests even with high proportions of sawdust. Such a result was associated with modern low-NOx-burners used in the Naantali boiler. In addition, the author concluded that co-firing could reduce CO_2, SO_2, and, to some extent, NOx emissions. Overall, NOx emissions from co-firing can be higher than from pure coal combustion because the high moisture content of sawdust causes delayed ignition of coal flame.

Priyanto et al., 2017, conducted a demonstration test of co-firing 25% woody biomass (energy basis) with coal in a 150-MW class pulverized coal boiler, in Japan. The objective was to investigate the effect of co-firing on the corrosion of boiler tubes. The authors used a modified coal mill to pulverize wooden pellets and then supplied the material to the boiler through four biomass burners. The co-firing process was observed to proceed stably without a reduction in the boiler efficiency. The authors confirmed that SOx and NOx emissions, measured at the exit of the furnace, were reduced proportionally to the co-firing ratio. In addition, they concluded that co-firing produced two to three times more alkali sulfates than pure coal firing and increased the ratio of unburned carbon in the deposits, the latter indicating a strongly reducing atmosphere in the furnace wall during co-firing. Moreover, co-firing increased locally the corrosion rate of furnace wall temperatures, especially in tubes located near biomass burners, which was associated with the locally reducing atmosphere and high amount of unburned carbon in initial deposits. However, no effect on the corrosion of superheater tubes was noticed.

2.3 ANALYSIS OF THE COMBUSTION BEHAVIOR OF SOLID FUELS IN LABORATORY

The combustion of solid fuels is a process that involves heat and mass transfer with chemical reactions and fluid flow. Understanding how biomass properties can influence biomass decomposition during combustion is crucial to obtaining more efficient fuel conversion. Among the methods for studying the combustion behavior of solid fuels, thermogravimetric analysis (TGA) and drop tube furnaces are very popular.

2.3.1 Thermogravimetric analysis

TGA is a technique, extensively used to investigate thermal reactions of solid fuels, that measures weight loss as a function of the furnace temperature of a small quantity of fuel exposed to a low heating rate with high precision and resolution [Pereira, Martins and Costa, 2016]. According to Barbieri, 2013, TGA is also widely used to evaluate the influence of particle size, sample mass, heating rate, and reactant gas in the fuel's reactivity. In addition, some quantitative methods can be applied to TGA curves to obtain kinetic parameters. However, the resultant reactivity parameters obtained with TGA do not represent well the combustion process that occurs in large-scale systems, which Manquais et al., 2009, associated with the combustion rate being a result of three interacting factors. Those factors are the intrinsic reaction rate of the internal surface of the fuel particles, the size of this surface, and the intensity to which oxygen diffuses through the pores. Nevertheless, TGA-based experiments provide convenient, rapid, and quantitative means to analyze sample mass changes during combustion, which can be a suitable analytical choice for an initial prediction of combustion in industrial applications. TGA can provide relevant information about thermal stability, heats of decomposition, ignition temperatures, and reaction kinetics of solid fuels, and is especially useful to comparative purposes.

Haykiri-Acma and Yaman, 2009, co-fired low-quality Turkish coals with woody shells of sunflower seed using the TGA method. Burnouts of five Turkish lignites were compared to burnouts of their blends with 10-20% biomass. The authors found that the combustion of mixtures ends in a shorter time compared to those from pure lignites. However, the addition of sunflower seed shells played different roles in the burnouts achieved by the Turkish coals. For one coal, the burnout increased with a rising share of biomass in the blends, while for the other coals the final burnout decreased to some extent. Nevertheless, these decreases in burnout may be tolerated because they did not seriously worsen the burnout behavior of the coals.

Wang et al., 2013, investigated the effects of biomass ratios, coal types, biomass types, and furnace temperature on the combustion and NO emission characteristics of pulverized coals and biomass blends using a TGA system. The authors found that biomass addition increased the burning rate and reduced the burnout time compared to pure coal. Concerning NO emission, the increase of biomass ratio increased de NO-releasing rate but reduced the final NO conversion ratio. The final NO conversion of samples was associated with the total volatile content in the samples because the conversion ratio of fuel-N to NO decreases with the rise of the volatile content. The volatiles in the biomass fuels used in their study were much higher than in the coal.

Mortari et al., 2018, studied the interaction effects between sugarcane bagasse and Brazilian coal during co-firing regarding the interference of the bagasse volatiles content in the coal thermal decomposition (activation energy and ignition temperature). Thermal decomposition behavior analyses were evaluated during co-firing using different biomass ratios in a thermogravimetric balance. The authors concluded that the ignition of coal was improved by the ignition of the high volatile biomass used because the ignition temperature of blended fuels decreased as the ratio of sugarcane bagasse increased. In addition, the kinetic data indicated that the burnout of blends might be improved by the interactions between both fuels compared to pure coal because of the high volatile content of sugarcane bagasse.

2.3.2 Drop tube furnace

DTF simulates better the industrial conditions in the combustion process of solid fuels by creating an environment that is possible to reach short residence times, high temperatures, fast heating rates, and dilute particle phases [Manquais et al., 2009]. While in TGA the gas-solid reactions occur at heating rates lower than 100 °C min^{-1} and residence times in magnitudes of minutes to hours, in DTF solid particles are exposed to heating rates around 10^4-10^5 °C min^{-1} and residence times of milliseconds to few seconds, as stated in Moço et al., 2017. Generally, the DTF is bench-scale equipment consisting of a vertical furnace electrically heated with the walls' temperatures monitored by thermocouples. Fuel particles and air are continuously fed into the furnace. According to Pereira, Martins and Costa, 2016, DTFs have been mainly used to study solid fuel ignition, flame stability, and burnout. Many authors have investigated the effects of co-firing coal and biomass using a drop tube furnace. Some of them will be discussed below.

Spliethoff and Hein, 1998, explored the effects of co-combustion of bituminous coal and different types of biomass and sewage sludge on emissions in coal-fired systems regarding the dependence on the fuel type. Their study also investigated the impact of various particle sizes on burnout. The authors concluded that the complete burnout depends both on the residence time at high temperatures and on the size of the particles, which means that the burnout decreased when residence times were not sufficient or the biomass particles were too coarse. Concerning emissions, they found that CO emissions can be correlated with burnout directly, which means the addition of biomass did not lead to an increase in CO emission compared with coal firing, as long as the biomass was ground to a small size. In addition, during unstaged combustion, the NOx emissions of blends with straw, Miscanthus, and wood decreased with a rising share of biomass. The NO_x emissions of sewage sludge were very high, which was attributed to the decrease in temperature due to the high ash content of sewage sludge. Moreover, the authors found that increasing biomass share led to a strongly decreasing in SO_2 emissions probably because the sulfur content on biomass was lower than in coal. Another reason attributed by the authors could be the change in conversion rate of biomass, which means that the more biomass was injected, the more sulfur was captured in the ashes. For sewage sludge, sulfur capture in the ash was not observed.

Kruczek, Rczka and Tatarek, 2006, presented an investigation on the co-combustion of hard and brown coal with different types of biomass. Tests were conducted in an electrically heated flow reactor to determine the effect of combustion temperature and the impact of biomass addition on the level of pollutant formation and burnout. The authors observed that the combustion blends of coal and biomass showed slightly higher temperatures near the burner than pure coal, which they associated with the increase of volatile content with the addition of biomass because the pyrolysis starts earlier for biomass fuels. Moreover, the addition of biomass resulted in a decrease in NOx and SO_2 emissions, but to different degrees, demonstrating a strong dependence on the particle size and type of coal and biomass. The emissions of NOx and SO_2 increased with the increase in temperature, but for finer particles, the differences were negligible. They also found that burnout increased with the increase in biomass ratio and the magnitude of this effect was dependent on the type of coal and biomass.

Kwong et al., 2007, investigated the combustion performance and gaseous pollutant emissions during co-combustion of rice husk and bamboo with pulverized coal in a laboratory-scale testing facility. The authors found that a general decrease in temperature occurred with the increasing of the biomass-blending ratio (BBR) due to the different heating values of the biomass blend. The minimum pollutant emission factors normalized by the energy output was

found within a range of 10-30% BBR. They also considered the effect of biomass grinding size on combustion performance. Pulverized coal in the grinding range of 75-106 µm and biomass with grinding sizes within the ranges of 106-150 µm, 150-212 µm, and 300-425 µm were used in the experiments. The authors concluded that the biomass grinding size did not seem to have a significant impact on either the combustion performance or the combustion temperature and the various pollutant emissions.

Sarkar et al., 2014, performed a comparative study of the combustion performance of two blends using TGA and DTF experiments: one blend of coal and raw sawdust and another blend of coal and sawdust char. The authors identified that the burnout efficiency of both blends was higher than that of pure coal, but they did not observe a straightforward correlation with the increase in the proportion of biomass (raw or char) in the mixtures, especially near the fuel injection point. They associated this result with the rapid combustion of volatile matter giving rise to a competition for oxygen molecules. Blends prepared with sawdust char demonstrated more synergistic effect on ignition performance during co-combustion in addition to giving more heat input (heat energy per unit mass) and ease of grind/feed than blends prepared with raw sawdust.

Rokni et al., 2018, studied the gaseous emission of carbon, sulfur, and nitrogen oxides as well as hydrogen chloride acid gases from co-firing coal with corn straw and rice husk (both their raw and torrefied states) in a DTF. The authors found that combustion efficiencies for the torrefied biomass were higher when compared to the raw biomass. They associated this result with the fact that torrefied biomass was less fibrous than raw biomass and its particles had lower aspect ratios. In addition, rice husk presented higher combustion efficiencies than corn straw, which was also attributed to its lower aspect ratio when compared to the corn straw particles. Concerning gaseous emissions, they identified that CO_2 emissions for all blends were lower than for pure coal and torrefied biomass in the blends generated higher CO_2 emissions than raw biomass. The authors attributed such disparities to the differences in the bulk equivalence ratios among the fuel samples and to differences in their carbon contents. For all blends, SO_2 emissions were lower than those of pure coals probably because of the higher sulfur retention in the alkali-rich ashes from biomass fuels. Regarding NOx emissions, the authors observed lower emissions for blends of coal and biomass when compared to pure coals, which they associated with different conversion pathways for the fuel nitrogen. In addition, the NOx emissions from torrefied biomass blends were higher than those from raw biomass because the torrefaction process increased the mass fraction of nitrogen content of fuels.

Sh et al., 2019, investigated the combustion behavior of one biomass fuel and two types of coal using a thermogravimetric analyzer and a DTF, considering the effects of particle, stoichiometric air ratio, and blending ratio on co-firing. Concerning DTF tests, the authors found that when fine particles of wood pellets (WP) were blended with two different types of coal, an oxygen deficiency in the early stage developed because of rapid combustion. Moreover, they did not detect a correlation between combustion behavior and biomass-blending ratio. In other words, the combustion efficiency did not change at the same level as the biomass ratio increased. For example, when WP fuel containing the smallest particle size was applied to the blend with the bituminous coal, the combustion efficiency decreased compared to pure coal. On the other hand, when the WP particle size increased, the combustion efficiency improved. They also identified that coarse particle blends demonstrated a decrease in combustion efficiency because of the slower reactivity associated with large particles.

Ashraf, Sattar and Munir, 2022, studied the co-combustion of coal and agricultural residues in a DTF in terms of burnout efficiency, NO_x, SO_2, and CO emissions. The authors noticed that biomass addition in coal blends reduced NOx emissions because of mainly two reasons. The first reason was the high volatile matter of agricultural residues, which increased devolatilization resulting in a low rate of NOx formation due to the rapid consumption of oxygen during this stage. The other reason was that the ash content of biomass is rich in basic metal oxides, resulting in NOx reduction to N_2 during char combustion. They also observed that an increase in biomass share resulted in an increased rate of NOx reduction. In addition, co-firing performed a positive impact on the emission of SO_2, which was associated with two reasons: the low sulfur content of biomass fuels, which reduced the overall sulfur content in the mixture with coal, and the higher amount of alkali and alkaline earth metal oxides present in biomass ash, which captured the oxides of sulfur from combustion gases. Moreover, the authors found lower emissions of CO and higher burnout for all blends compared to the combustion of pure coal.

Some authors have also investigated the differences between the combustion behavior of solid fuels using both thermogravimetric analysis and drop tube furnaces experiments. Manquais et al., 2009, compared the reactivity of chars from bituminous coal generated in DTF to those generated from TGA. A detailed investigation of the effects of temperature and coal particle size and the impact of char type was conducted. The authors found that the mean burnout rates from TGA and DTF chars were correlated for small particle sizes (< 75 µm), but for coarse particles (> 75 µm), the TGA chars became less combustible than those from DTF, which was associated with differences in char morphologies. While DTF char samples were

highly porous and extensively swollen, TGA char samples were heterogeneous, sharp-edged, and angular. Therefore, the DTF chars had larger internal surface areas, suggesting that the availability of surface-active sites is crucial in determining TGA burnout rates.

Moço et al., 2017, examined the combustion behavior of three distinct coals using thermogravimetric analysis and drop tube furnace experiments. The authors also evaluated the kinetic parameters of the three coals by following a model-fit approach using TGA tests. They concluded that the burnout values obtained in the DTF correlate well with the apparent activation energy evaluated from the non-isothermal TGA data. In other words, the lower the activation energy, the higher the burnout. However, the kinetic parameters extracted from TGA cannot directly explain the combustion behavior of the coals in the DTF because of the differences in the mechanisms that control the reactions in each technique. In TGA experiments, volatiles release and burning are likely to occurr before the char combustion, while the volatiles release may simultaneously occur with the char oxidation in the DTF.

3. MATERIALS AND METHODS

Some chemical and physical aspects of five biomass fuels were analyzed to determine their potential in co-combustion with coal in a DTF. Of these, SATC - Associação Beneficente da Indústria Carbonífera de Santa Catarina was responsible for evaluating proximate analysis, ultimate analysis, calorific value, and ash composition of the fuels. Sample preparation, ash fusibility, ignition temperature, and chlorine content were performed in the Laboratório de Siderurgia (LASID) of the Universidade Federal do Rio Grande do Sul (UFRGS). The DTF used for combustion and gas emissions analysis was placed in the Laboratório de Combustão of UFRGS. The materials and methods used in these analyzes are presented in this chapter.

3.1 SAMPLE PREPARATION

Brazilian coal CE5000 was used pulverized as received from the supplier. The biomasses selected for technical evaluation were: sawdust (SW), pine chips (PI), eucalyptus chips (EU), rice husk (RH), and sugarcane bagasse (SB).

Biomass fuels were received in very large particle sizes, so grinding was required to achieve the ideal size for the analyses performed. Therefore, biomasses were mixed and quartered in samples of 1 kg in a riffle box. Then a small riffle box (Figure 3.1) was used to obtain samples of 250 g, which were used in the following steps.

Figure 3.1 – Riffle box.

3.1.1 Evaluation of biomass grindability

This analysis identified complications that could occur during grinding biomass fuels in a cutting mill. Since no standard procedure was found for this type of analysis, the adopted procedure was based on equipment available in the laboratory.

The initial particle size distributions of the fuels were determined by sieving. The sieves were assembled in the sieve shaker (Figure 3.2) with screens of the following aperture sizes: 19 mm, 10 mm, 4 mm, 2 mm, 1 mm, 0.85 mm, 0.5 mm, and 0.25 mm. About 100 g of biomass was sieved at a time for 10 minutes in maximum vibration intensity until the whole sample of 250 g was done. The mass of biomass retained in each sieve was recorded to determine particle size distribution.

Figure 3.2 – Sieves assembled in the sieve shaker.

After that, biomasses were passed through the cutting mill (Figure 3.3), which was composed of a rotor with cutting tools mounted under its shaft, so when the rotor was turned, the cutting edges of the tools ground the material. The material was collected in a box after passing through a sieve. Biomass was hand-feed through an opening at the top of the cutting mill. For sawdust, rice husk, and sugarcane bagasse, a sieve with an aperture of 2 mm was used

in the cutting mill, because they have small initial particle sizes. For pine and eucalyptus chips, which have large initial particle sizes (above 19 mm), samples were passed twice through the mills. In the first pass, a sieve with an aperture of 10 mm was used, and in the second pass, a sieve with an opening of 2 mm was used.

Figure 3.3 – Cutting mill SM 100 from RETSCH.

3.2 FUEL CHARACTERIZATION

For chemical characterization, biomasses were ground to particle sizes smaller than 1000 μm, which represents the opening size of the last sieve through which all particles passed. Fuels characterization was performed to identify which fuels would be more suitable for the co-combustion process by comparing their physicochemical characteristics.

3.2.1 Chemical characterization

The chemical characterization was performed for all raw biomasses and coal.

- Proximate Analysis: Determination of moisture, volatile matter, and ash and the calculation of fixed carbon on fuels, according to ASTM D3172, ASTM D3173, ASTM D3174, and ASTM D3175.
- Ultimate analysis: Determination of carbon, nitrogen, hydrogen, sulfur, and oxygen content of fuels, according to ASTM D5373 for C, H, and N, and ASTM D4239 for S.
- Gross calorific value: Measurement of the amount of heat released per mass unit from the fuel by either an isoperibol or adiabatic bomb calorimeter, according to ASTM D5865-13.

3.2.2 Characterization of ashes

Ashes of pure fuels were characterized to identify their major species and to determine their fusibility behavior according to the following procedures.

- Ash composition: Determination of major and minor components in ashes of solid fuel using X-ray fluorescence spectrometry. Samples were prepared with the loss on ignition tests according to ASTM D7348-07.
- Ash fusibility: Determination of the melting behavior of solid fuel ash produced in an oxidizing atmosphere following the standard procedure DIN 51730. The principle of the test consisted in identifying critical temperature points, which were the initial deformation temperature (DT), the formation spherical temperature (ST), the hemispherical temperature (HT), and the fluid temperature (FT). Ashes of biomass and coal were obtained according to the standard procedures ASTM D3174-12 and ASTM E1755-01. A cylindrical specimen was created from the ashes. The specimen was placed in a heating microscope and heated until 1500 °C, while its shape was recorded by the microscope over time.

In addition, the ashes of two mixed fuel samples were analyzed to check if any interaction between ashes from two different fuels were likely to happen with respect to fusibility characteristics. Thus, two distinct samples were prepared with selected biomasses, one containing 50% of coal CE5000 and 50% of sawdust and the other containing 50% of coal CE5000 and sugarcane bagasse, both on a mass basis. The ashes of these mixed fuels were obtained following the same procedure as pure fuels.

3.2.3 Ignition temperature

The analysis followed the experimental procedure presented by Tognotti et al., 1985, using a thermogravimetric technique. A thermobalance was used to measure the weight loss of the samples. A 30 mg sample was placed on a 6 mm crucible which was immersed in an oxidant (air) and inert (N_2) environment with gas temperatures continuously monitored by a thermocouple near the sample. A 10°C/min heating rate was maintained constant until the environment temperature reached 900°C. The technique consisted in comparing weight-temperature plots obtained in oxidant and inert atmospheres for each sample. The ignition temperature was taken as the gas temperature at which the curves separate.

3.2.4 Chlorine content

This analysis determined the total chlorine in fuels by the ion-selective electrode method according to ASTM D4208-19. The method consisted in combusting a 1 g sample in an oxygen combustion vessel with a dilute base adsorbing the chlorine vapors. The vessel and the crucible were rinsed in a beaker with deionized water. An ionic strength adjuster was added to the beaker. An ion-selective electrode determined the chlorine content.

3.3 Estimation of CO_2 emissions from combustion of biomass

The calculations used in this analysis estimated possible changes in CO_2 emissions in the replacement of coal with biomass only based on the ultimate analysis and the heating values of biomasses. This calculation was relevant only to estimate the quantity of CO_2 observed in the chimney and did not include the whole biomass life cycle, which should account for handling, storage, transportation, and other aspects that can cause an impact on CO_2 emissions. In addition, an estimation of the maximum reduction potential of CO_2 emissions considering neutral emissions from biomass was determined.

The potential CO_2 formation was determined from the carbon content in fuels for pure coal, pure biomass, and mixtures from 5% to 30% of coal substitution according to Equation 3.1,

$$CO_{2,m} = X_b\, CO_{2,b} + (1 - X_b)\, CO_{2,coal} \tag{3.1}$$

where X_b is the mass ratio of biomass in the mixture and $CO_{2,i}$ is the generated carbon dioxide content from each fuel (kg_{CO2}/kg_{fuel}), which is given by Equation 3.2. The subscripts *m*, *b*, and *coal* refer to mixture, biomass, and pure coal, respectively.

$$CO_{2,i} = N_{C,i}\, M_{CO2} \tag{3.2}$$

where M_{CO2} is the molar mass of carbon dioxide ($kg_{CO2}/kmol_{CO2}$) and $N_{C,i}$ is the carbon molar content of each fuel ($kmol_C/kg_{fuel}$) given by,

$$N_{C,i} = W_{C,i}/M_C \tag{3.3}$$

where $W_{C,i}$ is the carbon content on each fuel (kg_C/kg_{fuel}), M_C is the molar mass of carbon ($kg_C/kmol_C$).

Substitution of coal was determined on an energy basis, that is, the amount of biomass on a mass basis that supplies the same energy generated by the portion of coal that is replaced. Equation 3.4 presents the mass of biomass needed in coal-biomass mixtures,

$$m_b = Y_{sub}\, m_{coal,0} \left(\frac{LHV_{coal}}{LHV_b}\right) \tag{3.4}$$

where m_b is the mass of biomass (g) necessary in the mixture that generates the same power by the original mass of pure coal, $m_{coal,0}$ (g), Y_{sub} is the ratio of coal substitution on energy basis, and *LHV* is the lower heating value of fuels (kJ/kg). Thus, the mass ratio of biomass needed in the mixture is given by,

$$X_b = \frac{1}{1 + \frac{LHV_b}{LHV_{coal}}\left(\frac{1}{Y_{sub}} - 1\right)} \tag{3.5}$$

The development of Equations 3.4 and 3.5 is shown in more detail in Appendix A.

3.4 COMBUSTION ANALYSIS

3.4.1 Coal-biomass blends

Sawdust and sugarcane bagasse were selected to proceed to experimental tests in DTF based on the results obtained from the characterization and logistical and economic aspects evaluated by Braskem teamwork involved in the project. The main reason for choosing these fuels was the availability of suppliers to provide the amount of biomass needed for Braskem's boilers. Test conditions were defined as presented in Figure 3.4 for each biomass.

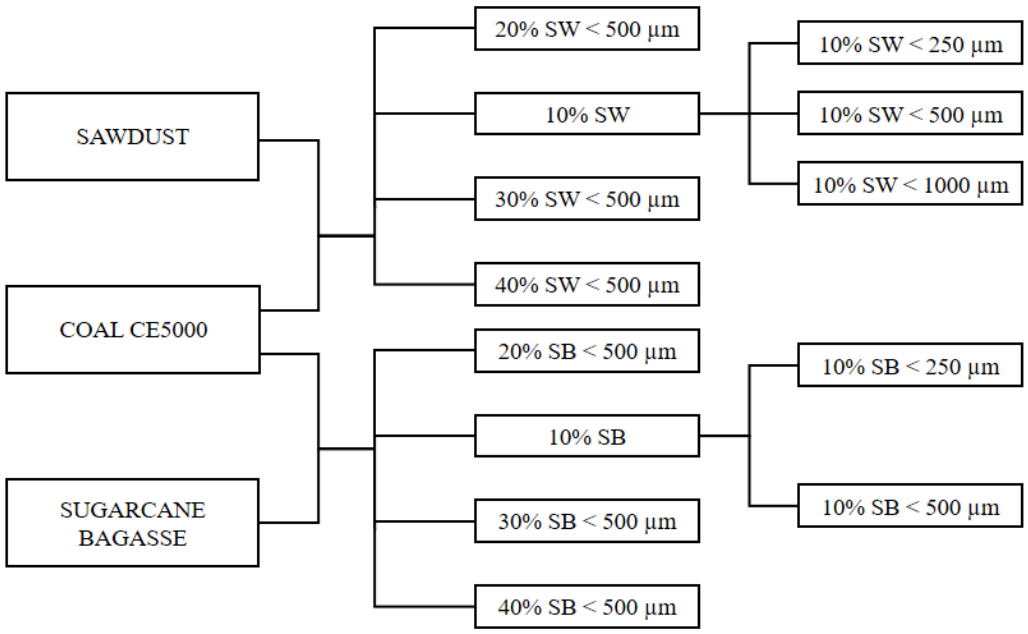

Figure 3.4 – Sample composition scheme for testing in DTF.

First, pulverized coal was mixed with sawdust and sugarcane bagasse in a fixed proportion of 10% of biomass on an energy basis. For combustion analysis, three different size bands were adopted, so biomasses were ground to particle sizes smaller than 1000 µm, 500 µm, and 250 µm. The tests performed with these three different particle sizes figured out the effect of particle size on the burnout behavior of blended fuels compared to burnout from pure coal. After that, sawdust and sugarcane bagasse were quartered and blended with pulverized coal to generate progressive shares of 10%, 20%, 30%, and 40% of the biomass in the mixture with particle sizes below 500 µm. The effect of biomass addition in the blend with coal can be

determined from these tests, i.e., how combustion efficiency of the mixed fuel behaves compared to pure coal. Coal and biomass blending ratios were determined based on energy compensation for the portion of coal replaced by biomass.

3.4.2 Drop tube furnace

The experiments were conducted in a drop tube furnace constructed in the Combustion Laboratory at UFRGS, as shown in Figure 3.5. The DTF is composed of a cylindrical ceramic tube with an inner diameter of 48 mm and a length of 1600 mm surrounded by three concentric tubular furnaces that are electrically heated. During tests, nine type-K thermocouples continuously monitored the wall temperatures. The maximum equipment temperature is 1200 °C.

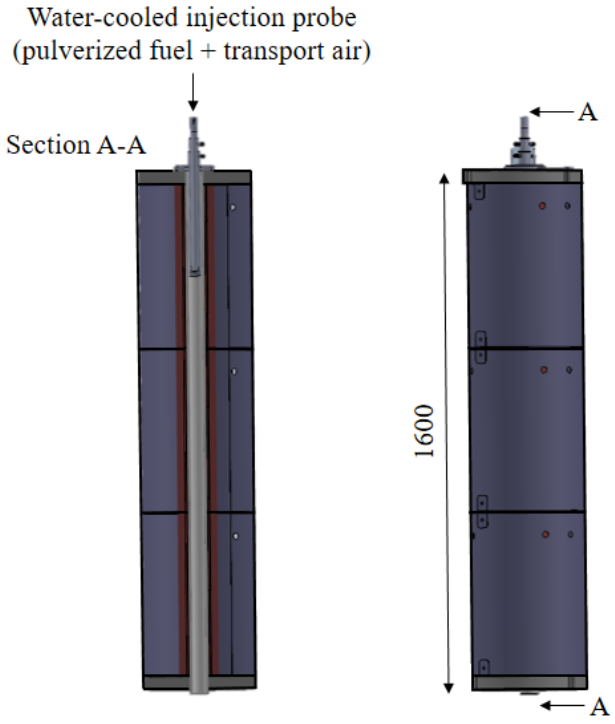

Figure 3.5 – Schematic of the DTF used in experimental tests.

A water-cooled injector, placed at the top of the DTF, was used to feed solid fuels and air into the combustion chamber. A pneumatic feeder (Figure 3.6) injected solid fuels into the DTF within an airflow that is responsible for dragging the particles. The feeder consists of a glass tube with an inner diameter of 20 mm where solid fuels were placed. The air was injected

through another tube concentric with the glass tube. The air injection tube is movable and has its speed regulated by an electronic controller connected to a small electric motor next to the glass tube. The air injection tube moved down as the screw attached to the electric motor rotated to ensure alignment between the air outlet and the fuel level. The electronic controller was set to maintain screw rotation at 13 revolutions per second.

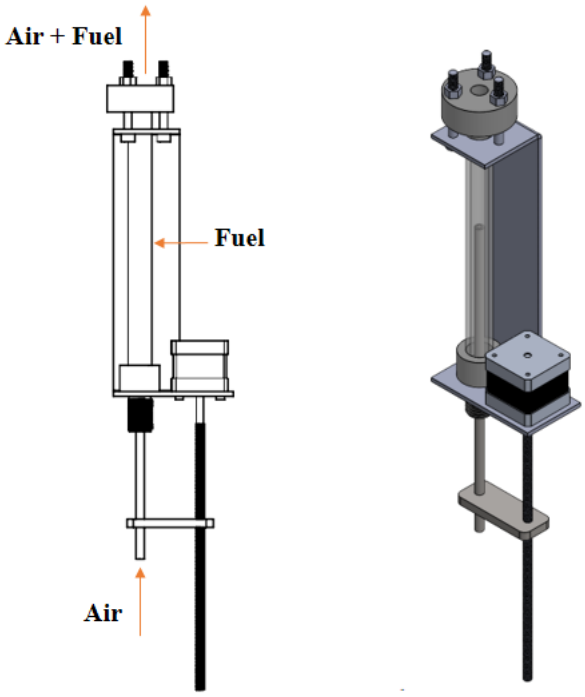

Figure 3.6 – Schematic of the DTF pneumatic feeding system.

A tube connected at the outlet of the feeder led fuel particles and air into the DTF (Figure 3.7). Fuel particles went through the combustion process along the furnace axis. Partially burned particles (char) were collected at different distances from the injection point along the furnace axis with a probe. The probe consists of four concentric stainless steel tubes. Nitrogen circulates between the walls of the two innermost tubes and exits through 8 holes in the smaller tube to quench the burning reaction. Water circulates between the walls of the two outermost to cool the probe (Figure 3.8). Char was collected inside the innermost tube aspirated by a vacuum pump. A quartz filter retained char samples between the probe exit and the vacuum pump. The samples were placed in an oven at approximately 60 °C to dehydrate and then analyzed. Each condition was repeated at least three times to guarantee statistical representativeness of the results.

Figure 3.7 – Feeding system connected to the fuel injector at the top of the DTF.

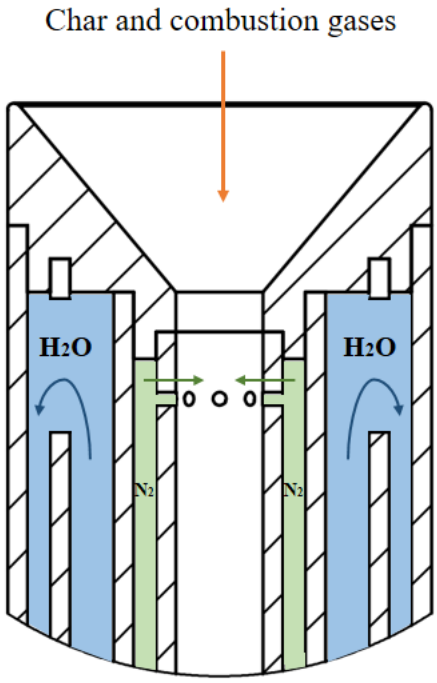

Figure 3.8 – Schematic of the water-cooled probe.

3.4.3 Stoichiometric air-fuel ratio

The stoichiometric air-fuel ratio is the amount of oxidizer needed to completely burn a quantity of fuel. According to Turns, 2012, the stoichiometric air-fuel ratio can be found as,

$$(A/F)_{stoic} = \left(\frac{m_{air}}{m_{fuel}}\right) \tag{3.6}$$

where m_{air} and m_{fuel} are the mass of the air and fuel, respectively, and $(A/F)_{stoic}$ is the stoichiometric air-fuel ratio.

The stoichiometric fuel ratio in mass was determined by calculating the oxygen necessary to completely burn carbon, hydrogen, and sulfur existing in the fuel. The fuel oxygen content was discounted. Since oxygen represents 23.3% of the mass of the air, the stoichiometric air-fuel ratio can be found as,

$$(A/F)_{stoic} = 4{,}292\ (2{,}667C + 8H + S - O) \tag{3.7}$$

where *C*, *H*, *S*, and *O* are the elemental composition by mass of carbon, hydrogen, sulfur, and oxygen of the fuel, respectively. The development of Equation 3.7 presented in Appendix A.

3.4.4 Burnout analysis

During the experiments, DTF wall temperatures were maintained at 900 °C. The pneumatic feeder transported the fuel particles with a primary airflow rate of 11 L/min, which represented about 80% of the total air passing through the furnace. The secondary air flow rate (4 L/min) was injected directly into the furnace. Air was injected into the DTF at room temperature. The division between primary and secondary air was determined to avoid a recirculation zone inside the combustion chamber without impairing the dragging of particles.

Along the furnace axis, char samples were collected with the probe at 400 mm, 500 mm, and 700 mm, distances measured from the fuel injector outlet. The combustion efficiency (burnout) was calculated according to the ash-tracer method,

$$Burnout = \left[1 - \left(\frac{Ash_{fuel}}{100 - Ash_{fuel}}\right)\left(\frac{100 - Ash_{char}}{Ash_{char}}\right)\right]100 \quad (3.8)$$

where *Burnout* is the combustion efficiency of fuel (%), Ash_{fuel} is the ash content of fuel at the injection point (%), and Ash_{char} is the ash content of the samples at the distance of sample collection (%). The detailed development of Equation 3.8 is presented in Appendix A.

3.4.5 Gas emissions analysis

For gas emissions analysis, a tube was installed at the exit of the vacuum pump, and probes were connected to the tube to lead combustion gasses to the gas analyzers.

The SIEMENS Ultramat 23 gas analyzer, which measured levels of O_2, CO, CO_2, NO, and SO_2, was used to analyze combustion gases. Specific sensors read the emission levels of each component and the Agilent Bench Data Logger 3 linked to the analyzer recorded the data. Gas reading started about 1 minute after starting feeding in the DTF. The software was set to record emission levels every 200 milliseconds for 8 minutes straight. Thereafter, the results of the recorded data were verified and the emission level for each component was determined as the average of an interval of those 8 minutes when measurements were sufficiently stable. The accuracy of the SIEMENS Ultramat 23 gas analyzer is shown in Table 3.1.

Table 3.1 – Accuracy of the SIEMENS Ultramat 23 gas analyzer.

Parameter	Accuracy	Operating range
Oxygen (O_2)	± 1%	0 - 100%
Carbon monoxide (CO)	± 10 ppm	0 - 1000 ppm
Carbon dioxide (CO_2)	± 0.2%	0 - 20%
Nitric oxide (NO)	± 10 ppm	0 - 1000 ppm
Sulfur dioxide (SO_2)	± 5 ppm	0 - 500 ppm

In parallel, the KANE 940 gas analyzer was used to corroborate the results found by the SIEMENS analyzer. KANE 940 measured the levels of O_2, CO, NO, and SO_2. In this case, after

the first minute of feeding in the DTF, results were read in the front panel of the KANE analyzer and registered every minute, and then compared with the average of results found by the SIEMENS analyzer in the same time interval. The accuracy of the KANE 940 gas analyzer is shown in Table 3.2.

Table 3.2 – Accuracy of the KANE 940 gas analyzer.

Parameter	**Resolution**	**Accuracy**	**Operating range**
Oxygen (O_2)	0,1%	± 0.2%	0 - 21%
Carbon monoxide (CO)	1 ppm	± 20 ppm < 400 ppm ± 5% < 5000 ppm ± 10% > 5000 ppm	0 - 10000 ppm
Nitric oxide (NO)	1 ppm	± 5 ppm < 100 ppm ± 5% > 100 ppm	0 - 1000 ppm
Sulfur dioxide (SO_2)	1 ppm	± 5 ppm < 100 ppm ± 5% > 100 ppm	0 - 500 ppm

The concentration of chemical species in combustion gases depends directly on air excess used during combustion because of the dilution of pollutants compared to stoichiometric burning. Thus, a comparison of emission levels independent of air excess was achievable using a correction of species concentration to a predetermined level of O_2 given by Equation 3.9 presented by Carvalho Jr. and Lacava, 2003,

$$Y_{i,corr} = \left(\frac{0{,}21 - Y_{O2,corr}}{0{,}21 - Y_{O2,md}}\right) Y_{i,md} \tag{3.9}$$

where $Y_{i,corr}$ is the concentration level corrected for species i, $Y_{O2,corr}$ is the oxygen level chose for correction, $Y_{O2,md}$ is the oxygen level measured during the combustion, and $Y_{i,md}$ is the concentration level measured for species i during the combustion. In this work, all species concentrations were corrected to 6% of oxygen level.

5. CONCLUSIONS

This study initially investigated the chemical and physical characteristics of five biomass fuels to identify their potential performance in co-combustion with Brazilian coal (CE5000). The biomasses investigated were sawdust (SW), pine chips (PI), eucalyptus chips (EU), rice husk (RH), and sugarcane bagasse (BS). Based on this previous investigation, two biomasses were selected to examine their combustion characteristics with coal regarding the effects of different biomass particle sizes and proportions. The main conclusions can be summarized as follows:

- Grind PI and EU to small sizes was complicated because of the large number of particles with large dimension (> 19 mm). SW, RH, and SB were easy to grind.
- Regarding biomass composition, they presented high volatile content and low ash content, except for RH. The nitrogen content was about half of the coal for SW, PI, RH, and SB, but it was higher for EU, which could be a disadvantage since nitrogen content is closely related to NOx emissions. Sulfur was not detected in any biomass evaluated, reinforcing the benefit of biomass in potentially reducing SOx emissions.
- Compared to coal, biomass ash presented more elements typical of plants, such as calcium, magnesium, and potassium. SW, EU, PI, and RH ash did not show fusion characteristics below 1500 °C, while SB ash started to deform at 1250 °C. However, fusibility tests with samples containing 50% coal and 50% SW or 50% SB demonstrated initial deformation at 1450 °C.
- The ignition temperature of all biomass fuels was lower than that of coal, which can be explained by their high volatile content. Lower ignition temperature of biomass can lead to anticipated steps of devolatilization and combustion of coal.
- EU, PI, and SB showed the lowest values for chlorine content, which is a positive aspect since chlorine could be associated with deposit formation and corrosion. On the other hand, the chlorine content of SW and RH was about three times higher than that of coal.
- The analysis of the potential formation of CO_2 indicated a rise in CO_2 formation with the increase in biomass ratio for EU, RH, and SW. The opposite effect was observed for PI and SB because of PI's high LHV and SB's low carbon content.
- Some advantages and disadvantages were observed in chemical and physical characterization of all biomasses. Therefore, sawdust and sugarcane bagasse were selected for combustion analysis based mainly on logistical and economic aspects

evaluated by the teamwork from Braskem. Nonetheless, continuous use of sawdust for combustion requires analyzing emissions of toxic components such as dioxins and furans and monitoring the integrity of the boiler pipes more regularly because of the high chlorine content in sawdust.

- Mixtures with 10% SW < 250 µm and < 500 µm reached burnout values statistically equal to pure coal burnout and converged to maximum burnout at the same point as coal. However, for the coarse particle size sample (<1000 µm) a downward trend in burnout behavior was observed, which was associated with the biomass particle size about ten times larger than coal, considering the PSD analysis.
- Mixtures with 10% SB showed a tendency to decrease combustion efficiency increasing biomass particle size to < 500 µm, while samples with particle size < 250 µm showed similar burnouts than coal. This behavior was also associated with the large aspect ratio of this type of biomass due to its fibrous structure.
- SW < 500 µm was blended with coal in proportions of 10%, 20%, 30%, and 40%. Although the burnout behavior of blends did not show a linear tendency with the addition of biomass, as the residence time increased, all coal-SW blends demonstrated a tendency to reach maximum burnout. These results can be explained by the oxygen deficiency caused by finer particles and slower reactivity due to coarse particles.
- SB < 500 µm was blended with coal in proportions of 10%, 20%, 30%, and 40%. All burnout values were lower than that of pure coal and a tendency to decrease in burnout was noticed with the increase of biomass ratio, which was associated with the large dimension of SB particles. Large particles will take more time to heat, dry, and ignite, even if they contain high volatiles.
- Generally, blending SW with coal until 40% of biomass on an energy basis, with biomass particle size < 500 µm, proved to be most viable and more beneficial than blending SB with coal in any proportion with the same granulometry. SW mixtures did not negatively influence or did not significantly change burnout compared with pure coal burnout.
- Comparing predicted and measured burnouts of coal-SW blends, the actual burnout values for the mixture with SW particles < 500 µm were mostly close to the theoretical ones or higher. On the other hand, for the mixture with SW particles under 1000 µm, the burnout values measured after the combustion in DTF were much lower than the

predicted ones, which was also attributed mainly to the presence of biomass particles with large aspect ratios.

- Emissions from blends with both SW and SB were complex and did not show a clear trend in their behavior with the increase in biomass ratio. Nonetheless, for all blends, CO levels converged to low values at the maximum burnout point, and the NO emitted was close or lower than that of pure coal. In addition, a tendency to decrease SO_2 emissions was observed with the increase of biomass share, which was expected due to the low sulfur content in SW and SB. CO_2 emissions increased compared to pure coal probably because SW and SB have LHV lower than coal. However, the final balance on CO_2 emissions requires a more detailed and individualized evaluation of the biomass life cycle.
- Generally, considering the coal maximum burnout point, emissions of CO and NO from SB blends were higher than those from SW. Emissions from SW were very close to coal emissions. However, the combustion process inside the DTF occurred at a relatively low temperature (900 °C) and with a high excess of air to drag fuel particles to the furnace. Therefore, the emissions found in the DTF may not represent the actual conditions in industrial furnaces.

5.1 SUGGESTIONS FOR FURTHER WORKS

From the experience acquired in the development of this work and the results obtained, some suggestions for further works are:

- Verification of fuel ash conservation along the DTF and its peripherals to identify possible problems that may cause segregation of blended fuels in the feeding and collecting systems of the DTF;
- Morphological analysis of coal and biomass to investigate further the effect of particle size difference during co-combustion;
- Chemical kinetic analysis of combustion of pure and blended fuels through computational modelling;
- Expansion of co-combustion studies to other types of biomass, other furnace wall temperatures and more char collection points in the DTF.

REFERENCES

Agbor, E., Zhan, X. and Kumar, A. A review of biomass co-firing in North Americ. **Renewable and Sustainable Energy Reviews**, vol. 40, p. 930-943, 2014.

Al-Mansour, F. and Zuwala, J. An evaluation of biomass co-firing in Europe. **Biomass and Bioenergy**, vol. 34, p. 620-629, 2010.

American Society for Testing and Materials. **ASTM D3172:** Standard Practice for Proximate Analysis of Coal and Coke. ASTM International, West Conshohocken, PA, 2021.

American Society for Testing and Materials. **ASTM D3173/D3173M:** Standard Test Method for Moisture in the Analysis Sample of Coal and Coke. ASTM International, West Conshohocken, PA, 2017.

American Society for Testing and Materials. **ASTM D3174:** Standard Test Method for Ash in the Analysis Sample of Coal and Coke from Coal. ASTM International, West Conshohocken, PA, 2018.

American Society for Testing and Materials. **ASTM D3175:** Standard Test Method for Volatile Matter in the Analysis Sample of Coal and Coke. ASTM International, West Conshohocken, PA, 2020.

American Society for Testing and Materials. **ASTM D4208:** Standard Test Method Total Chlorine in Coal by the Oxygen Vessel Combustion/Ion Selective Electrode Method. ASTM International, West Conshohocken, PA, 2019.

American Society for Testing and Materials. **ASTM E1755:** Standard Test Method for Ash in Biomass. ASTM International, West Conshohocken, PA, 2020.

Ashraf, A., Sattar, H. and Munir, S. A comparative performance evaluation of co-combustion of coal and biomass in drop tube furnace. **Journal of the Energy Institute**, vol. 100, p. 55-65, 2022.

Barbieri, C. C. T. **Estudos de misturas de carvões e biomassa visando a combustão em alto-forno**. Dissertação de mestrado, Universidade Federal do Rio Grande do Sul, 2013.

Bashir, M. S., Jensen, P. A., Frandsen, F., Wedel, S., Dam-Johansen, K., Wadenbäck, J. and Pedersen, S. T. Ash transformation and deposit build-up during biomass suspension and grate firing: Full-scale experimental studies. **Fuel Processing Technology**, vol. 97, p. 93-106, 2012.

Basu, P. **Combustion and Gasification in Fluidized Beds**. CRC Press, Boca Raton, 1st edition, 2006.

Baxter, L. Biomass-coal co-combustion: Opportunity for affordable renewable energy. **Fuel**, vol. 84, p. 1295-1302, 2005.

Baxter, L. Biomass-Coal cofiring: an Overview of Technical Issues. In: Grammelis, P. (editor). **Solid biofuels for energy: A lower greenhouse gas alternative**, Springer-Verlag, London, 2011.

Branco, V. and Costa, M. Effect of particle size on the burnout and emissions of particulate matter from the combustion of pulverized agricultural residues in a drop tube furnace. **Energy Conversion and Management**, vol. 149, p. 774-780, 2017.

Carvalho Jr, J. A. and Lacava, P. T. **Emissões em Processos de Combustão**. Editora UNESP, São Paulo, 2003.

Coelho, P. and Costa, M. **Combustão**. Editora Orion, Portugal, 1ª edição, 2007.

Demirbas, A. Potential applications of renewable energy sources, biomass combustion problems in boiler power systems and combustion related environmental issues. **Progress in Energy and Combustion Science**, vol. 31, p. 171-192, 2005.

EPE. Balanço Energético Nacional – BEN 2021. **Empresa de Pesquisa Energética**, p. 268, 2021.

Gil, M. V. and Rubiera, F. Coal and Biomass cofiring. In: Suárez-Ruiz, I., Diez, M. A. and Rubiera, F. (editors). **New Trends in Coal Conversion: Combustion, Gasification, Emissions, and Coking**, Woodhead Publishing, 2019.

Glassman, I., Yetter, R. A. and Glumac, N. G. **Combustion**. Elsevier, 5th edition, 2015.

Gomes, A. P., Ferreira, J. A. F., Albuquerque, L. F. and Süffert, T. Carvão fóssil. **Estudos**

Avançados, vol. 12, p. 89-106, 1998.

Haykiri-Acma, H. and Yaman, S. Effect of biomass on burnouts of Turkish lignites during co-firing. **Energy Conversion and Management**, vol. 50, p-2422-2427, 2009.

Hein, K. R. G. and Bemtgen, J. M. EU clean coal technology – Co-combustion of coal and biomass. **Fuel Processing Technology**, vol. 54, p. 159-169, 1998.

IEA. **Coal 2021**. Available at https://www.iea.org/reports/global-energy-review-2021/coal. 2021a. Accessed in March, 2022.

IEA. **Global Energy Review 2021**. Available at https://www.iea.org/reports/global-energy-review-2021. 2021b. Accessed in March, 2022.

IEA BIOENERGY. **Database of Biomass Cofiring initiatives**. Available at: https://task32.ieabioenergy.com/database-biomass-cofiring-initiatives. 2017. Accessed in June, 2022.

IPCC. Summary for Policymakers. In: **The Physical Science Basis. Contribution of Work I to the Sixth Assessment Report of the Intergovernmental Panel on Climate Change** [Masson-Delmotte, V., P. Zhai, A. Pirani, S.L. Connors, C. Péan, S. Berger, N. Caud, Y. Chen, L. Goldfarb, M. I. Gomis, M. Huang, K. Leitzell, E. Lonnoy, J.B.R. Matthews, T.K. Maycock, T. Waterfiel, O. Yelekçi, R. Yu, and B. Zhou (eds.)]. In Press, 2021.

Jiang, Y., Mori, T., Naganuma, H. and Ninomiya, Y. Effect of the optimal combination of bituminous coal with high biomass content on particulate matter (PM) emissions during co-firing. **Fuel**, vol. 316, 2022.

Kalkreuth, W., Holz, M., Kern, M., Machado, G., Mexias, A., Silva, M. B., Willett, J., Finkelamn, R. and Burger, H. Petrology and chemistry of Permian coals and from the Paraná Basin: 1. Santa Terezinha, Leão-Butiá and Candiota Coalfields, Rio Grande do Sul, Brazil. **International Journal of Coal Geology**, vol. 68, p. 79-116, 2006.

Kruczek, H., Rczka, P. and Tatarek, A. The effect of biomass on pollutant emission and burnout in co-combustion with coal. **Combustion Science and Technology**, vol. 178, p. 1511-1539, 2006.

Kwong, P. C. W., Chao, C. Y. H., Wang, J. H., Cheung, C. W. and Kendall, G. Co-

combustion performance of coal with rice husks and bamboo. **Atmospheric Environment**, vol. 41, p. 7462-7472, 2007.

Manquais, K., Snape, C., McRobbie, I., Barker, J. and Pellegrini, V. Comparison of the combustion reactivity of TGA and drop tube furnace chars from a bituminous coal. **Energy and Fuels**, vol. 23, p. 4269-4277, 2009.

Merrick, D. **Coal Combustion and Conversion Technology**. Macmillan, London and Basingstoke, 1st edition, 1984.

Moço, A., Costa. M., Casaca, C., Pohlmann, J. G. and Pereira, F. M. Combustion Behavior of Coals from Thermogravimetric and Drop Tube Furnace Experiments. In: **10th Mediterranean Combustion Symposium**, Naples, Italy, 2017.

Mortari, D. A., Torquato, L. D. M., Crespi, M. S. and Crnkovic, P. M. Co-firing of blends of sugarcane bagasse and coal: Thermal and kinetic behaviors. **Journal of Thermal Analysis and Calorimetry**, vol. 132, p. 1333-1345, 2018.

Pedersen, L. S., Nielsen, H. P., Kiil, S., Hansen, L. A., Dam-Johansen, K. D., Kildsig, F., Christensen, J. and Jespersen, P. Full-scale co-firing of straw and coal. **Fuel**, vol. 75, p. 1584-1590, 1996.

Pereira, S., Martins, P. C. R. and Costa, M. Kinetics of Poplar Short Rotation Coppice Obtained from Thermogravimetric and Drop Tube Furnace Experiments. **Energy and Fuels**, vol. 30, p. 6525-6536, 2016.

Priyanto, D. E., Matsunaga, Y., Ueno, S., Kasai, H., Tanoue, T., Mae, K. and Fukushima, H. Co-firing high ratio of woody biomass with coal in a 150-MW class pulverized coal boiler: Properties of the initial deposits and their effect on tube corrosion. **Fuel**, vol. 208, p. 714-721, 2017.

Pronobis, M. Evaluation of the influence of biomass co-combustion on boiler furnace slagging by means of fusibility correlations. **Biomass and Bioenergy**, vol. 28, p. 375-383, 2005.

Riaza, J., Gibbins, J., and Chalmers, H. Ignition and combustion of single particles of coal and biomass. **Fuel**, vol. 202, p 650-655, 2017.

Rokni, E., Ren, X., Panahi, A. and Levendis, Y. A. Emissions of SO2, NOx, CO2, and HCl from Co-firing of coals with raw and torrefied biomass fuels. **Fuels**, vol. 211, p. 363-374, 2018.

Roni, M. S., Chowdhury, S., Mamum, S., Marufuzzaman, M., Lein, W. and Johson, S. Biomass co-firing technology with policies, challenges, and opportunities: A global review. **Renewable and Sustainable Energy Reviews**, vol. 78, p.1089-1101, 2017.

Sahu, S.G., Chakraborty, N. and Sarkar, P. Coal-biomass co-combustion: An overview. **Renewable and Sustainable Energy Reviews**, vol. 34, p. 575-586, 2014.

Sami, M., Annamalai, K. and Wooldridge, M. Co-firing of coal and biomass fuel blends. **Progress in Energy and Combustion Science**, vol. 27, p. 171-214, 2001.

Sarkar, P., Sahu, S. G., Mukherjee, A., Kumar, M., Adak, A. K., Chakraborty, N. and Biswas, S. Coal-combustion studies for potential application of sawdust or its low temperature char as co-fuel with coal. **Applied Thermal Engineering**, vol. 63, p. 616-623, 2014.

Savolainen, K. Co-firing of biomass in coal-fired utility boilers. **Applied Energy**, vol. 74, p. 369-381, 2003.

Sh, L., Jeong, T., Jeon, K., Park, K., Lee, B. and Jeon, C. Combustion behaviors of wood pellet fuel and its co-firing with different coals. **Journal of Mechanical Science and Technology**, vol. 33, p. 4545-4553, 2019.

Spliethoff, H., Hein, K. R. G. Effect of co-combustion of biomass on emissions in pulverized fuel furnaces. **Fuel Processing Technology**, vol. 54, p. 189-205, 1998.

Suárez- Ruiz, I., Diez, M. A. and Rubiera, F. Coal. In: Suárez-Ruiz, I., Diez, M. A. and Rubiera, F. (editors). **New Trends in Coal Conversion: Combustion, Gasification, Emissions, and Coking**, Woodhead Publishing, 2019.

Tognotti, L., Malotti, A., Petarca, L. and Zanella, S. Measurement of ignition temperature of coal particles using a thermogravimetric technique. **Combustion Science and Technology**, vol. 44, p. 15-28, 1985.

Turns, S. R. **An Introduction to Combustion: Concepts and Applications**. 3rd edition, McGraw-Hill, New York, 2012.

Vassilev, S. V., Baxter, D., Andersen, L. K and Vassileva, C. G. An overview of the chemical composition of biomass. **Fuel**, vol. 89, p. 913-933, 2010.

Yadav, S. and Mondal, S. S. A complete review based on various aspects of pulverized coal combustion. **International Journal of Energy Research**, v. 43, p. 3134-3165, 2019.

Zuwala, J. and Lasek, J. Co-combustion of low-rank coals and biomass. In: Luo, Z. and Agraniotis, M. (editors). **Low-Rank Coals for Power Generation, Fuel and Chemical Production**. Woodhead Publishing, 2017.

Wang, C., Wang, J., Lei, M. and Gao, H. Investigations on combustion and NO emission characteristics of coal and biomass blends. **Energy and Fuels**, vol. 27, p. 6185-6190, 2013.

Wang, G., Silva, R. B., Azevedo, J. L. T., Martins-Dias, S. and Costa, M. Evaluation of the combustion behavior and ash characteristics of biomass waste derived fuels, pine and coal in a drop tube furnace. **Fuel**, v. 117, p. 809-824, 2014.

APPENDIX A – CALCULATION MEMORY

Coal substitution:

The ratio of biomass needed in the mixture for coal substitution is given by,

$$X_b = \frac{m_b}{m_m} \tag{A.1}$$

where the mass of biomass, m_b, and the mass of coal-biomass mixture, m_m, are defined as,

$$m_b = \frac{E_b}{LHV_b} \tag{A.2}$$

$$m_m = m_b + m_{coal} \tag{A.3}$$

where E_b is the amount of energy generated by the biomass in substitution of coal, which is obtained from the amount of energy generated by pure coal, $E_{coal,0}$,

$$E_b = Y_{sub}\, E_{coal,0} \tag{A.4}$$

The amount of energy generated by each type of fuel is given by,

$$E_i = m_i\, LHV_i \tag{A.5}$$

Combining Equations A.2, A.4, and A.5, the Equation 3.4 is obtained,

$$m_b = Y_{sub}\, m_{coal,0} \left(\frac{LHV_{coal}}{LHV_b}\right) \tag{3.4}$$

where $m_{coal,0}$ is the original mass of pure coal. The mass of coal in the mixture is given by,

$$m_{coal} = m_{coal,0}\,(1 - Y_{sub}) \tag{A.6}$$

Combining Equations A.1, A.3, A.6, and 3.4, the Equation 3.5 is obtained,

$$X_b = \frac{1}{1 + \frac{LHV_b}{LHV_{coal}}\left(\frac{1}{Y_{sub}} - 1\right)} \tag{3.5}$$

Stoichiometry:

The stoichiometric air fuel ratio is determined by writing simple atom balances, assuming that the fuel reacts to form an ideal set of products, given by the following reactions:

$$C + O_2 \rightarrow CO_2 \tag{A.7}$$

$$2H + 1/2\, O_2 \rightarrow H_2O \tag{A.8}$$

$$S + O_2 \rightarrow SO_2 \tag{A.9}$$

$$2O \rightarrow O_2 \tag{A.10}$$

The air necessary to completely burn each reaction is,

$$\left(\frac{m_{O_2}}{m_{fuel}}\right)_c = \frac{1\, M_{O_2}}{1\, M_C}\left(\frac{kg_{O_2}}{kg_C}\right) c \left(\frac{kg_C}{kg_{fuel}}\right) = \frac{32}{12} c \left(\frac{kg_{O_2}}{kg_{fuel}}\right) = 2{,}667c \tag{A.11}$$

$$\left(\frac{m_{O_2}}{m_{fuel}}\right)_h = \frac{1/2\, M_{O_2}}{1\, M_H}\left(\frac{kg_{O_2}}{kg_H}\right) h \left(\frac{kg_H}{kg_{fuel}}\right) = \frac{(1/2)\ 32}{(2)\ 1} h \left(\frac{kg_{O_2}}{kg_{fuel}}\right) = 8c \tag{A.12}$$

$$\left(\frac{m_{O_2}}{m_{fuel}}\right)_s = \frac{1\, M_{O_2}}{1\, M_S}\left(\frac{kg_{O_2}}{kg_S}\right) s \left(\frac{kg_S}{kg_{fuel}}\right) = \frac{32}{32} s \left(\frac{kg_{O_2}}{kg_{fuel}}\right) = s \tag{A.13}$$

$$\left(\frac{m_{O_2}}{m_{fuel}}\right)_o = -o \tag{A.14}$$

where *M* indicates the atom molar mass, and the subscripts *C*, *H*, *S*, and *O* identify carbon, hydrogen, sulfur, and oxygen atom, respectively. Therefore, the total amount of oxygen needed for complete combustion is given by,

$$\left(\frac{m_{O2}}{m_{fuel}}\right) = \left(\frac{m_{O2}}{m_{fuel}}\right)_c + \left(\frac{m_{O2}}{m_{fuel}}\right)_h + \left(\frac{m_{O2}}{m_{fuel}}\right)_s - \left(\frac{m_{O2}}{m_{fuel}}\right)_o \quad (A.15)$$
$$= 2{,}667c + 8h + s - o$$

Oxygen represents 23.3% of the mass of the air, so the stoichiometric air-fuel ratio is given by,

$$(A/F)_{stoic} = \left(\frac{m_{air}}{m_{fuel}}\right) = \frac{1}{0{,}233}\left(\frac{m_{O_2}}{m_{fuel}}\right) \quad (A.16)$$

Combining Equations A.15 and A.16, the Equation 3.7 is obtained,

$$(A/F)_{stoic} = 4{,}292\ (2{,}667C + 8H + S - O) \quad (3.7)$$

Burnout:

The burnout is defined as the loss of fuel during its combustion and it was determined using the ash tracer method. Therefore, the burnout can be expressed as the ratio of the combustible mass fraction remaining in the char at the collection point and the combustible mass fraction available to be burned in the initial fuel mass, that is,

$$Burnout = \frac{(VM_{char} + FC_{char})\,\dot{m}_{char}}{(VM_{fuel} + FC_{fuel})\,\dot{m}_{fuel}} \quad (A.17)$$

where FC_{fuel} and VM_{fuel} are, respectively, the initial content of fixed carbon and volatiles in the fuel, and FC_{char} and VM_{char} are the fixed carbon and volatile content in the collected char. The combustible part of a fuel can be written as,

$$FC_i + VM_i = 1 - Ash_i \quad (A.18)$$

One assumption of ash tracer technique is that ash fraction in the fuel is not affected during combustion. Therefore,

$$Ash_{fuel}\,\dot{m}_{fuel} = Ash_{char}\,\dot{m}_{char} \tag{A.19}$$

Combining Equation A.17, A.18 and A.19,

$$Burnout = 1 - \left[\left(\frac{1 - Ash_{char}}{1 - Ash_{fuel}}\right)\frac{Ash_{fuel}}{Ash_{char}}\right] \tag{A.20}$$

Rearranging Equation A.20, the Equation 3.8 is obtained,

$$Burnout = \left[1 - \left(\frac{Ash_{fuel}}{100 - Ash_{fuel}}\right)\left(\frac{100 - Ash_{char}}{Ash_{char}}\right)\right]100 \tag{3.8}$$

Ash char:

The char collected with the probe was retained in a quartz-filter. The filter with char were deposited in a crucible that was placed in a drying oven at approximately 70 °C during 15 minutes. After that, the sample was measured in an analytical balance to determine the initial mass of the char,

$$m_{char,i} = m_{sample} - m_{cruc} - m_{filt} \tag{A.21}$$

where:

$m_{char,i}$ = initial mass of dried sample (g),

m_{sample} = mass of dried sample, crucible, and filter (g),

m_{cruc} = mass of crucible (g),

m_{filt} = mass of dried filter (g).

Then, the sample was placed in a muffle to completely burn following the procedures of ASTM D3174-12 for coal and coal-biomass blends and ASTM E1755-01 for pure biomass. Then, the ash content in the char sample collected was calculated as,

$$Ash_{char} = \left(\frac{m_{ash,char} - m_{cruc} - m_{filt}}{m_{char,i}} \right) \quad \text{(A.22)}$$

where:

$m_{ash,char}$ = mass of ash, crucible, and filter, (g).